Eksploatacja i Niezawodnosc - Maintenance and Reliability

Volume 29 (2027), Issue 1

https://ein.org.pl

The Polish Maintenance Society

Bi-objective dynamic group maintenance optimization for a heterogeneous two-component system with bidirectional coupling and economic dependence: a rolling time-domain approach based on NSGA-II

Jiawei Liu[1], Mengze Qin[1], Bing Bing[1], Chiming Guo[1,*]

[1] Shijiazhuang Campus, Army Engineering University, China
* Corresponding Author: guochiming@aeu.edu.cn

Received: 7 May 2026
Revised: 3 June 2026
Accepted: 9 June 2026
Online: 15 July 2026

Abstract

Existing studies on multi-component maintenance often model component dependence as unidirectional, homogeneous, or independent, which limits their ability to capture bidirectional interactions and their impact on maintenance decisions. This paper proposes a dynamic grouped maintenance optimization model for a heterogeneous two-component system with bidirectional degradation coupling and economic dependence. The model minimizes the long-run system cost rate and unavailability under finite system life and limited maintenance resources. A rolling-horizon method based on NSGA-II is developed to obtain Pareto maintenance decisions at each inspection point, and the model is validated through simulations. Under the same coupling strength, the proposed strategy reduces the long-run cost rate by 26.99%, 10.29%, and 8.93%, and system unavailability by 29.13%, 15.25%, and 12.66%, respectively, compared with benchmark models. Sensitivity analysis further confirms its applicability and robustness, providing decision support for heterogeneous multi-component systems.

Keywords: *heterogeneous components, stochastic dependencies, economic dependencies, group maintenance, bidirectional coupling*

Article citation:
Liu J, Qin M, Bing B, Guo C, Bi-objective dynamic group maintenance optimization for a heterogeneous two-component system with bidirectional coupling and economic dependence: a rolling time-domain approach based on NSGA-II, Eksploatacja i Niezawodnosc – Maintenance and Reliability 2027: 29(1) http://doi.org/10.17531/ein/224350

Highlights

- Extend group maintenance to bidirectionally coupled heterogeneous systems.
- Model coupling via state coupling functions and equivalent age.
- Optimize dynamic grouping with waste-life and resource-shortage penalties.
- NSGA-II rolling horizon minimizes long-run cost rate and unavailability.
- The model cuts system cost by 26.99% and downtime by 29.13%.

1. Introduction

Maintenance refers to all technical and managerial activities carried out to maintain or restore components or systems to their specified functional state, and typically includes preventive maintenance, corrective maintenance, and maintenance based on condition or predictive information. As modern equipment systems evolve toward larger scales, greater complexity, and increased intelligence, they are typically composed of multiple components with differing structures, functions, and degradation mechanisms. These components are not only subject to mutual constraints in terms of cost, structure, and resources, but may also exhibit degradation correlations due to factors such as load, vibration, temperature, shock, or operating environments. Therefore, traditional maintenance strategies focused on single components or mutually independent components can no longer meet the comprehensive requirements of complex systems in terms of reliability, availability, maintenance costs, and resource constraints. In their review of multi-component maintenance, Nicolai and Dekker [1] point out that interactions among multiple components, while increasing the complexity of maintenance modeling and optimization, also provide opportunities for grouping maintenance activities and achieving cost savings—a core distinction between multi-component maintenance optimization and single-component maintenance optimization. Wildeman and Dekker [2,3] distinguish three types of dependencies in multi-component systems: economic dependency, structural dependency, and stochastic dependency. Economic dependency refers to the sharing of downtime, disassembly, preparation, or labor costs when multiple components are repaired together, thereby generating economic benefits from grouped or opportunistic maintenance. Studies such as references [4–7] indicate that opportunistic maintenance and grouped maintenance are the most effective methods for addressing economic dependencies. For example, early reviews on economic dependencies categorized multi-component maintenance models into steady-state and dynamic models, and further discussed the organization of maintenance activities from three perspectives: corrective maintenance grouping, preventive maintenance grouping, and combined preventive-corrective grouping. Structural dependency refers to assembly, disassembly, or functional interconnections between components, such that repairing one component may require the simultaneous disassembly or handling of other components. Regarding structural dependency (i.e., components in a system that are structurally or functionally constrained, such that repairing one component requires at least the disassembly or repair of other units). Olde et al. [8] distinguishes between performance dependencies and technical dependencies. Performance dependencies mean that different configurations of components affect the system's reliability and availability, while technical dependencies mean that repairing a given component requires or prohibits the repair of other components. Random dependencies emphasize that the degradation or failure of a component alters the degradation rate, failure probability, or remaining life of other components. Building on this, Olde et al. [8] identifies another type of dependency: resource dependency, which applies when multiple components depend on a shared set of spare parts or tools, or on a limited number of maintenance personnel. References [4, 9, 10] and others have considered the impact of resource dependency on maintenance strategies for multi-component systems, taking into account factors such as the number of maintenance personnel and spare parts inventory.

1.1. Literature review

From the perspective of dependency mechanisms, stochastic dependencies represent the most challenging class of problems in multi-component maintenance optimization. When the degradation or failure of one component alters the degradation processes of other components, system maintenance decisions are no longer a simple aggregation of individual component strategies; instead, they require simultaneous consideration of state evolution, failure propagation, and maintenance interactions. Olde Keizer et al. [8] distinguishes between three scenarios: damage caused by failure, load sharing, and common-mode degradation. Regarding failure-induced damage, Nguyen et al. [11] addresses the maintenance modeling problem for a two-component system consisting of a gradually degrading component and a component prone to sudden failure (e.g., due to impact), while Zhang et al. [12] investigates CBM for a system of n components selected from k under periodic inspection, taking into account failure-induced damage—that is, component failure triggers transient impacts that accelerate the degradation of the remaining components. Regarding load sharing, the primary focus is on how the degradation or failure of one component (or a group of homogeneous components) affects the failure or degradation of other components. For example, Wang et al. [13] proposes a two-tier CBM modeling method that captures stochastic dependencies through rate-rate interactions, Xu et al. [6] formulated this specific maintenance problem—where the degradation of a particular component is influenced by its adjacent components—as a factorized Markov decision process and developed a factorized value iteration algorithm to solve it. Regarding common-mode degradation, Zhang et al. [14] considers the impact of the operating environment on component degradation; the harsher the environmental conditions, the faster the degradation rate. Similarly, the problem is formulated as a Markov decision process, and an iterative approximation algorithm is used to obtain an acceptable maintenance strategy. Huynh et al. [15] develops a high-performance opportunistic predictive maintenance (PdM) model for n out of k failure systems that are jointly affected by the operating environment.

In terms of research subjects, existing studies on multi-component maintenance can be broadly categorized into three types. The first type focuses on maintenance optimization for homogeneous or nearly homogeneous systems. Such studies typically assume that system components share identical or similar degradation processes, failure distributions, or maintenance response mechanisms, facilitating solutions using renewal theory, Markov decision processes, threshold strategies, or opportunistic maintenance strategies, as described in the literature cited earlier. Such models are relatively straightforward to handle in terms of theoretical analysis and algorithm design, making them particularly suitable for standard reliability structures such as k-out-of-n systems, parallel systems, or series systems. However, in actual mechatronic systems, different components often possess distinct physical functions, material properties, load paths, and degradation mechanisms; simple isomorphic assumptions struggle to accurately capture the heterogeneous degradation behavior observed during system operation.

In real-world complex systems, it is clear that no system follows a single degradation process. In typical electromechanical coupling systems, the degradation behavior of components is usually heterogeneous [16–18]; for example, the failure behavior of Component A may follow a Weibull distribution, while that of Component B may follow a Gamma distribution (Gamma distribution). In such systems, not only do independent degradation processes exist between components, but mutual interactions may also trigger dependent degradation; for instance, the vibration of Component A may accelerate the degradation of Component B, and conversely, the performance decline of Component B may lead to an increase in the failure rate of Component A.

In recent years, an increasing number of studies have focused on multi-component systems composed of heterogeneous components. For example, Song et al. [19] investigated the reliability assessment of k-out-of-n systems with heterogeneous multi-state components and load sharing, proposing a novel state ordering method that significantly reduced the computation time for reliability and remaining useful life; Lu et al. [20] proposed an interactive component-level predictive maintenance (PdM) scheduling and system-level OM optimization for a Service Parts Management System (SP-MMS) with heterogeneous degrading critical components and economic and structural dependencies among them, to obtain the optimal OM set; Kivanç et al. [21] Investigated optimal maintenance strategies for systems with a large number of heterogeneous components over a finite service life, and developed a decomposition method to calculate optimal maintenance strategies and inspection intervals for components; Bautista et al. [22] Studied the maintenance optimization problem for multi-component systems composed of heterogeneous components requiring different maintenance operations, and proposed a strategy to coordinate condition-based maintenance (CBM), maintenance lead times, and inspection strategies for such heterogeneous systems; Bautista et al. [23] Proposed a hybrid maintenance strategy combining condition-based and age-based approaches for multi-component systems with heterogeneous components, taking into account imperfect maintenance, and employed semi-regenerative techniques to evaluate the optimal strategy. Kıvanç et al. [24] proposed a state-based maintenance model with two control thresholds for systems composed of multiple heterogeneous degrading components over a finite life cycle, optimizing planned maintenance intervals at the system level and determining preventive and semi-emergency maintenance thresholds at the component level. This study emphasizes that a finite life cycle better aligns with the practical needs of OEMs and high-end equipment service scenarios than the infinite life assumption, although it still primarily assumes that component degradation processes are independent of one another. Zhao et al. [25] studied multi-component systems with heterogeneous failure dependencies, proposed a framework for quantifying different failure dependencies between components, and optimized maintenance strategies based on Markov processes, demonstrating that heterogeneous dependencies significantly affect system availability and maintenance costs. Such research has advanced the modeling of maintenance for heterogeneous systems; however, most studies still focus primarily on unidirectional influences, failure dependencies, or statistical correlations, and the characterization of bidirectional coupled degradation caused by physical interactions between components remains insufficient.

With advancements in sensors, the Industrial Internet of Things (IIoT), and health management technologies, maintenance decision-making based on remaining useful life

(RUL) prediction, deep learning, and probabilistic degradation modeling has gradually become a hot research topic. For example, Zeng and Liang [26] proposed a dynamic predictive maintenance method for fleets of multi-component systems, embedding the RUL distribution obtained from probabilistic deep learning into rolling time-domain maintenance planning, and introducing "wasted residual values" to quantify the loss of residual value caused by premature replacement. He et al. [27] further investigated the optimization of condition-based maintenance (CBM) for multi-component systems, taking into account predictive information and degradation-induced efficiency losses, with the goal of leveraging predictive information to enhance system-level maintenance benefits. Geurtsen et al. [28] addressed maintenance decision-making for serial production lines by proposing a maintenance optimization framework based on digital twins and deep reinforcement learning (DRL) that simultaneously considers quality trends, equipment status, and buffer interactions. Experimental results demonstrate that this method significantly outperforms traditional scheduling rules and heuristic strategies. Tan et al. [29] addressed the need for engineering systems in military scenarios to maintain a satisfactory level of combat readiness to respond to unexpected missions. They proposed a state-based maintenance and spare parts optimization method for multi-unit multi-state systems (MSS) based on reinforcement learning (RL), aiming to minimize the long-term cost rate while considering combat readiness status and routine operational requirements. Such methods can fully leverage monitoring data and predictive information, but their effectiveness typically depends on data quality, model training conditions, and prediction accuracy. At the same time, many data-driven methods focus more on the prediction and scheduling of "when to repair," while integrated modeling of physical couplings between components, economic dependencies, limited maintenance resources, and multi-objective trade-offs still requires further development.

In addition to random dependencies, economic considerations and resource constraints are also key factors influencing multi-component maintenance decisions. In real-world maintenance scenarios, if multiple components are maintained within a similar time window, costs associated with downtime preparation, inspection, disassembly and reassembly, or personnel scheduling can be shared, thereby reducing total maintenance costs; however, including a component in a grouped maintenance schedule too early can result in a waste of its remaining service life. Therefore, the essence of grouped maintenance lies in balancing cost savings with the potential waste of service life. On the other hand, limited maintenance resources create competition among maintenance tasks. If there is a shortage of maintenance personnel, spare parts, or maintenance windows, the system may be forced to delay maintenance or bear a higher risk of unavailability. Recent research on multi-component CBM with finite lifetimes has begun to address factors such as downtime costs, scheduled maintenance, semi-urgent maintenance, and limited service cycles. However, most studies still focus solely on cost minimization or fail to simultaneously address the multi-objective trade-offs between component coupling degradation, grouping economics, resource constraints, and system unavailability, as exemplified in Reference [24].

In summary, existing research has laid an important foundation for the optimization of maintenance in multi-component systems, but the following shortcomings remain. First, many models are still based on the assumptions of homogeneous components or independent degradation, making it difficult to reflect the actual characteristics of mechatronic systems, where the degradation mechanisms of different components vary significantly. Second, existing research on heterogeneous systems has primarily focused on heterogeneous failure dependencies, unidirectional effects, or statistical correlations, with insufficient physical explanations for bidirectional coupled degradation. This makes it difficult to describe the dynamic feedback process in which changes in the state of Component A affect Component B, while the degradation of Component B, in turn, affects Component A. Third, existing studies on grouped maintenance mostly emphasize cost savings under economic constraints, while insufficiently considering the comprehensive trade-offs between the waste of remaining service life caused by premature maintenance, maintenance penalties resulting from resource shortages, and system unavailability. Fourth, many studies focus primarily on single-objective optimization; even when dynamic or rolling-horizon methods are employed, cost is often treated as the primary evaluation metric, with little consideration given to the two conflicting objectives of long-term cost rate and system unavailability.

1.2. Main work and contributions of this paper

Against this backdrop, this paper proposes a dynamic grouped maintenance optimization model for heterogeneous two-component systems characterized by bidirectional coupling degradation and economic dependence. Unlike existing studies focused on homogeneous systems, unidirectional dependencies, or systems with independent heterogeneous components, this paper starts from the physical degradation mechanisms of components and utilizes state coupling functions and equivalent age to characterize the dynamic interactions between heterogeneous components. At the same time, it combines age-based maintenance and condition-based maintenance to design differentiated maintenance strategies for components with different degradation characteristics. In terms of cost modeling, this paper introduces relative wasted lifetime, batching savings factors, and resource scarcity to quantify the lifetime loss caused by early batch maintenance, the economic benefits of joint maintenance, and the penalty costs resulting from limited maintenance resources. Regarding optimization objectives, this paper simultaneously considers the system's long-term cost rate and system unavailability, constructing a dual-objective dynamic maintenance optimization model to more comprehensively reflect the trade-off between economic efficiency and availability in real-world engineering systems.

To solve the aforementioned dual-objective dynamic optimization problem, this paper further proposes a rolling-time-domain optimization method based on NSGA-II. At each checkpoint, based on the component's current degradation state, equivalent age, and remaining maintenance resources, NSGA-II is used to search for Pareto-optimal maintenance decisions within a finite prediction window, and the system state is updated by rolling forward after executing the decision for the current stage. Compared to one-time static optimization methods, the rolling-time-domain method can dynamically adjust maintenance plans based on the latest degradation information, making it suitable for complex maintenance scenarios characterized by constantly updating states, finite lifecycles, and resource constraints. Compared to single-objective maintenance optimization, NSGA-II can obtain a non-dominant solution set between cost rate and unavailability, supporting decision-makers in selecting appropriate strategies based on risk preferences and maintenance resource conditions.

Specifically, while NSGA-II, gamma-process degradation modeling, equivalent age, and rolling-horizon optimization are individually established in the literature, their combination for bidirectional coupled heterogeneous systems under economic constraints has not been presented in prior studies. This statement is supported by recent literature on multi-component maintenance optimization: Nguyen et al. [5] and Xu et al. [6] discuss dynamic grouping and condition-based maintenance in multi-component systems, highlighting that prior works focus on single-objective or unidirectional interactions, whereas our framework integrates multiple components, bidirectional coupling, and economic dependencies in a multi-objective optimization setting.

Compared with existing literature, the main contributions of this paper are:

(1) Under constrained system lifespans and maintenance resources, this study extends traditional group maintenance problems to heterogeneous systems featuring bidirectional coupling and economic dependencies. The effectiveness of this extension is verified by sensitivity analysis under different coupling strengths, with the proposed strategy reducing the long-term cost rate by up to 26.99% and system unavailability by up to 29.13% compared with baseline strategies.

(2) From a physical perspective, a coupling degradation model is established for heterogeneous systems. Innovatively employing state coupling functions and equivalent age to describe complex dynamic coupling relationships among heterogeneous components, the validity of this model is confirmed by the degradation path comparison in Section 4.2, which accurately captures the bidirectional acceleration effect between mechanical and electronic components.

(3) A dynamic group maintenance model is established for systems with finite lifespans and maintenance resources, applying distinct maintenance strategies to heterogeneous components. Relative wasted lifespan and resource shortage metrics are defined to quantify group maintenance penalty costs. The superiority of this

model is verified by the 8.93% cost rate reduction and 12.66% unavailability reduction compared with the static group maintenance strategy.

(4) A rolling time-domain approach based on NSGA-II is proposed. It evaluates overall performance using long-term system cost rate and system unavailability as metrics, while solving for local optima within finite prediction windows at each decision point to achieve global optimization. The performance of this method is verified by the well-distributed Pareto front and stable convergence in Section 4.3.

To clarify the novelty and advantages of the proposed model, we first compare it with representative analogous models from recent literature, as shown in Table 1. Existing studies mainly focus on heterogeneous maintenance policies, failure dependence, load-sharing mechanisms, or opportunistic maintenance. In contrast, this study integrates bidirectional degradation coupling, heterogeneous maintenance strategies, economic dependence, limited maintenance resources, and bi-objective dynamic optimization into a unified grouping maintenance framework.

Table 1. Comparison with state-of-the-art analogous models.

Ref.	**Research object**	**Heterogeneity**	**Dependence**	**Method**	**Objective**	**Difference from this study**
Song and Liang (2025)	Heterogeneous (k)-out-of-(n):F load-sharing system	Multi-state heterogeneous components	Load-sharing dependence	Markov process; state ordering; phase-type method	Reliability and RUL evaluation	No maintenance optimization or resource constraint
Bautista et al. (2024)	Heterogeneous multi-component system	Degrading and non-degrading components	Opportunistic maintenance dependence	Gamma process; semi-regenerative process	Minimize maintenance cost	No bidirectional degradation coupling
Kivanç et al. (2024)	Multi-component series system with finite lifespan	ABM, CBM, and FBM components	Economic dependence	MDP; dynamic programming; decomposition	Minimize cost and downtime	No physical coupling among degradation processes
Lu et al. (2025)	Serial–parallel multi-station manufacturing system	Heterogeneous degradation components	Economic and structural dependence	RUL prediction; MILP	Optimize opportunistic maintenance grouping	Focuses on production-system dependence
Kıvanç et al. (2025)	Multi-component series system	Heterogeneous degradation parameters	Economic dependence	MDP; dynamic programming	Minimize maintenance cost	Considers CBM only; no ABM–CBM combination
Zhao et al. (2023)	Multi-component system with heterogeneous failure dependence	Non-identical components and dependence intensities	Failure dependence; load redistribution	CTMC / Markov process	Maximize availability and minimize life-cycle cost	No equivalent-age model or grouping benefit
Bautista et al. (2025)	Heterogeneous system with degrading and non-degrading components	Degradation-observable and age-dependent components	Opportunistic maintenance dependence	Delay-time model; Weibull distribution; semi-regenerative process	Minimize long-run cost rate	No bidirectional coupling or resource-constrained grouping
This study	Heterogeneous two-component series system	Different degradation and maintenance characteristics	Bidirectional degradation coupling and economic dependence	State-coupling function; equivalent-age model; NSGA-II rolling-horizon optimization	Minimize long-run cost rate and system unavailability	Considers bidirectional coupling, grouping benefit, wasted lifetime, and resource shortage

Notes: ABM, CBM, and FBM denote age-based maintenance, condition-based maintenance, and failure-based maintenance, respectively. RUL denotes remaining useful life. MDP denotes Markov decision process, CTMC denotes continuous-time Markov chain, and MILP denotes mixed-integer linear programming.

1.3. Limitations and extensibility of this paper

This study has the following limitations, which define the applicable boundary of the proposed model:

(1) This paper takes a two-component series heterogeneous system as the research object to focus on the bidirectional coupling mechanism, and has not been extended to complex multi-component systems with series-parallel structures;

(2) The model adopts the perfect monitoring assumption, and does not consider the measurement error and random uncertainty in the actual monitoring process;

(3) A deterministic cost model is adopted, and the stochastic fluctuation of maintenance cost and downtime loss in actual engineering is not considered;

(4) Numerical validation is carried out based on synthetic

data calibrated from real engineering parameters, and full-cycle industrial verification on real systems has not been completed.

Meanwhile, the model can be extended to multi-component complex systems, more complex coupling relationships, and more general industrial scenarios, which is further discussed in the conclusion section.

The remainder of this paper is structured as follows: Section 2 presents the research questions and hypotheses; Section 3 establishes the relevant models and proposes a solution; Section 4 provides numerical validation of the proposed models and methods, along with a parameter sensitivity analysis; and Section 5 presents the conclusions. The definitions of the terms used in this paper are provided at the end of the paper, and the research framework is illustrated in Figure 1.

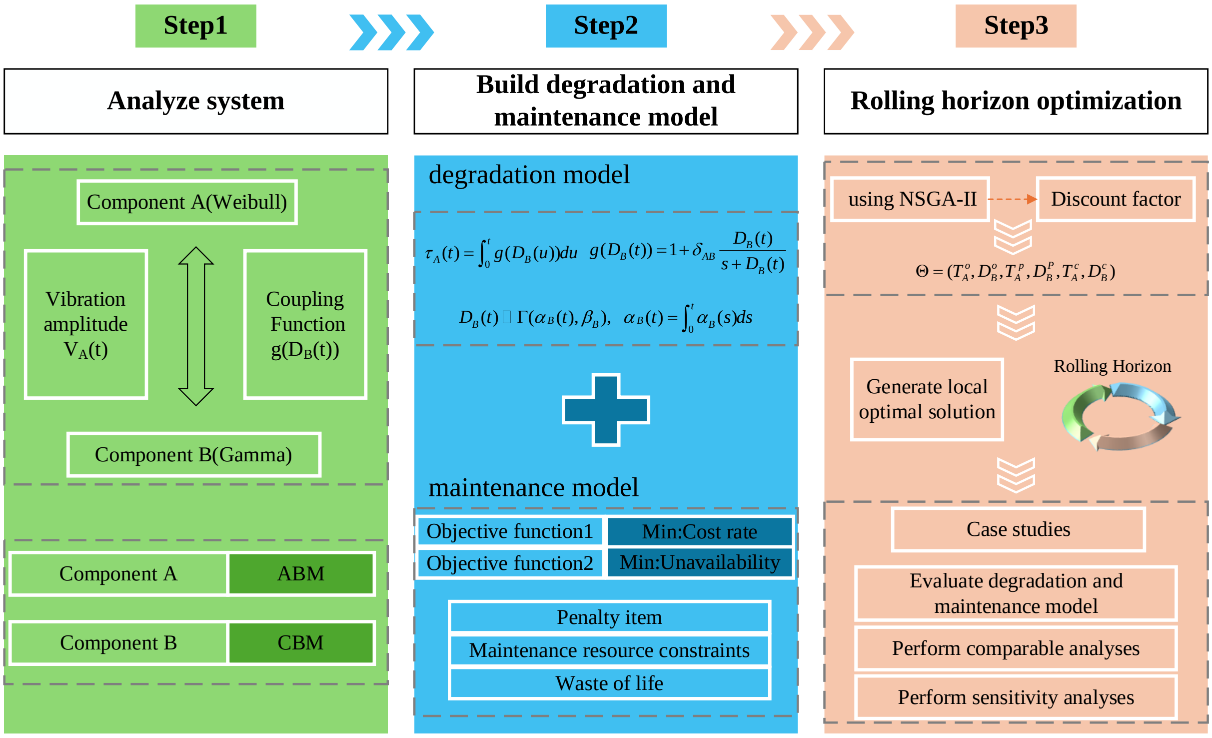

Figure 1. Research framework diagram.

2. Problem description and assumptions

2.1. Definition of systems and heterogeneous components

Consider a dual-component system composed of components connected in series, where failure of either component leads to system shutdown. This two-component heterogeneous system is the minimum core unit for studying bidirectional physical coupling in electromechanical systems, which is a classic research paradigm in the field of maintenance optimization [30,31]. The system is composed of two typical heterogeneous components widely existing in industrial scenarios: a mechanical part subject to fatigue wear and an electronic control unit subject to performance degradation, which corresponds to common equipment such as machine tool spindle-control system and wind turbine bearing-converter system, with strong engineering representativeness. The simplification to two components is to focus on the core bidirectional closed-loop coupling mechanism, avoiding the confusion of multi-component coupling relationships and the dimension explosion of decision space, while the core conclusions of the model can be extended to multi-component complex systems.

The system has a finite lifetime $T_S \in [0, T]$, with periodic inspections conducted at intervals of $\tau = T/K$, K denotes the number of inspections. The system comprises two heterogeneous components with distinct degradation types that interact: Component A is a mechanical part whose failure time follows a Weibull distribution. During normal operation, it generates slight vibrations whose amplitude increases with cumulative operating time. Component B is an electronic control unit whose degradation follows a gamma degradation process. During operation, it sends signals to Component A to execute corresponding actions, and its performance degrades as the degradation level increases.

To gain a clearer understanding of this heterogeneity, we use M_A and M_B to represent the failure times and degradation processes of components, $F_A(t)$ and $F_B(t)$ to denote the cumulative distribution functions of component failure or degradation, and θ_A, θ_B to roughly represent the component's own lifetime parameters. This heterogeneity can then be expressed in the following mathematical form: $H = \{M_A \neq M_B, F_A(t) \neq F_B(t), \theta_A \neq \theta_B, C_{A\to B} \perp\!\!\!\perp C_{B\to A}\}$. In this context, $C_{A\to B}$ and $C_{B\to A}$ represent the asymmetric coupling relationship between heterogeneous components. This two-component system was chosen to facilitate the study of maintenance strategies involving bidirectional coupling mechanisms and economic interdependencies. The two-component system provides a controlled framework that clearly illustrates the underlying principles without the complexity associated with multi-component systems.

2.2. Description of bidirectional coupling relationships

In multi-component systems, particularly complex systems composed of multiple heterogeneous components, the mutual influence between components cannot be overlooked. The degradation process of a component is not only affected by its own degradation mechanism but also influenced by other components.

In this paper, the coupling relationship between Component A and Component B manifests primarily in two aspects (For the specific mathematical formula, see Section 3.1.), collectively forming a closed-loop coupling chain within the system:

(1) Vibrations generated by Component A's operation accelerate Component B's degradation rate. Component A, being a mechanical part, typically produces vibrations that increase with its operating time. According to existing research such as [32] on vibration effects on surrounding electronic devices in mechanical systems, vibrations from Component A may damage or interfere with Component B (an electronic control unit), thereby accelerating its degradation process.

(2) Performance degradation of Component B increases the equivalent age of Component A, leading to excessive damage. As an electronic control unit, Component B's performance decline not only affects its own operational state but may also indirectly impact Component A's operating conditions, making Component A more susceptible to deterioration. For example, during degradation, Component B may experience reduced control precision, diminishing the accuracy and timeliness of control signals. This can subject Component A to greater mechanical shocks or unstable loads during operation, with such load variations significantly worsening Component A's condition [33]. The coupling relationship between the systems is illustrated in Fig. 2 below.

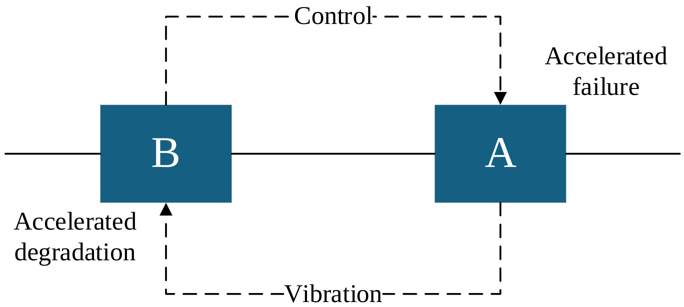

Figure 2. Coupling Relationship Diagram.

2.3. Component-level maintenance strategies

For maintenance strategies of heterogeneous components, Bautista et al. [23] proposed a hybrid approach combining condition-based maintenance (CBM) and age-based maintenance (ABM). Tailored to the characteristics of this paper, the maintenance strategy can optimize decisions based on the health status and operating time of different components.

(1) For mechanical component A (wear-fatigue component), maintenance primarily relies on an age-based (service-time-based) strategy, with maintenance triggered when the service time reaches a predetermined life threshold. Equivalent age refers to the operational lifespan of a repaired system, measured against a benchmark system, that would be required for the new system to achieve the same level of reliability. Note that tracking equivalent age becomes challenging when a component undergoes multiple maintenance actions [34]. Therefore, equivalent age is used solely to describe excess damage under coupled conditions. Maintenance decisions for Component A remain based on its actual usage age. This

approach is consistent with Brenière et al. [35]; it essentially simplifies the decision-making process and better aligns with real-world decision-making. Compared to the complex calculation of equivalent age, calendar age is more practical, facilitating rapid decision-making in practice, reducing unnecessary computation time, and improving maintenance efficiency.

(2) For electronic Component B (electrical control component), maintenance relies more heavily on condition-based strategies. Degradation levels are monitored to determine whether preventive maintenance thresholds or failure thresholds have been reached. Maintenance is performed only when the component's condition reaches a specific threshold. This strategy can accurately capture the real-time degradation state of electronic components through periodic inspection.

2.4. Grouped maintenance strategies under economic dependencies

Group maintenance is introduced to address the economic dependence between the two components. By performing maintenance on multiple components simultaneously, the setup cost and downtime can be shared, which can effectively reduce the total maintenance cost and system unavailability. The group supervision model in this paper adopts a simplified framework to focus on the core impact of bidirectional coupling and dynamic grouping on maintenance decisions. The model has covered the core logic of group maintenance, including opportunistic maintenance trigger conditions, maintenance opportunity windows, and penalty constraints for lifespan wastage and resource shortage. Maintenance costs can be shared when performing maintenance in groups [4,5,7], so grouping multiple maintenance activities can reduce overall maintenance expenses. Therefore, we are interested in constructing a grouped maintenance schedule that executes multiple maintenance activities to be optimized at each maintenance interval. However, it must be noted that when performing multiple maintenance activities at the same interval, maintenance costs may incur the following indirect penalties:

(1) If maintenance is performed ahead of scheduled preventive maintenance, the service life of the component will be relatively shortened.

(2) In actual maintenance activities, maintenance resources cannot always meet task requirements, resulting in cost penalties due to insufficient resources.

2.5. Basic assumptions of the model

Assumptions made for the current system:

- System components are inspected at fixed intervals, with each inspection perfectly detecting the component's degradation state, leading to either no maintenance or maintenance actions based on the state. The perfect monitoring assumption is a simplification to highlight the coupling and economic dependence, and monitoring uncertainties such as measurement errors will be considered in future study.
- The fixed inspection interval is determined according to the common inspection frequency of electromechanical systems and relevant literature, balancing the monitoring performance and inspection cost.
- The uncertainty existing in the actual monitoring process is recognized, which will be further addressed in the extended model.
- Components that fail between inspection intervals must wait until the next inspection time for maintenance.
- After preventive maintenance, the component’s state is restored to “new” condition.

3. Models and algorithms

This section primarily constructs a coupled degradation model to describe the complex coupling relationships among components. It proposes a dynamically updated dual-objective grouped maintenance model with distinct maintenance strategies for heterogeneous components, continuously optimized within a rolling time-domain framework.

3.1. Coupled degradation model

Based on the preceding description of coupling relationships and failure mechanisms among heterogeneous components within the system, the following physical model is established. Concepts such as coupling functions and equivalent age are employed to quantify the complex relationships between components as accurately as possible while approximating real-world conditions.

3.1.1. Failure model for component A

Component A is a mechanical component whose failure is dominated by fatigue and wear. The Weibull distribution is employed because it is the most widely used and appropriate model for mechanical fatigue failure. The failure time of Component A follows a Weibull distribution with a failure rate given by:

$$\lambda_{A0}(t) = \frac{m_A}{\eta_A}\left(\frac{t}{\eta_A}\right)^{m_A-1} \tag{1}$$

among these, $m_A > 1$ is the shape parameter, and $\eta_A > 0$ is the scale parameter. The operational state of Component A is influenced by the degradation level of Component B, analogous to the nonlinear cumulative damage model proposed for structures under variable load/stress conditions in material fatigue life analysis [36]. To describe this relationship, following [37, 38], we introduce the equivalent age of Component A to characterize the additional damage caused by the coupling effect of Component B on Component A. This reflects the degree of accelerated aging under the bidirectional coupling mechanism, rather than the actual operating time. We map the degradation amount $D_B(t)$ of component B through the coupling function $g(D_B(t))$ to an acceleration factor, which represents the failure rate of component A relative to its operating time without the influence of component B's degradation. Therefore, the equivalent age of component A at time t is given by the following equation:

$$\tau_A(t) = \int_0^t g(D_B(u))\,du \tag{2}$$

$\tau_A(t)$ is not the actual runtime of Component A, but rather its equivalent usage time compared to an uncoupled state, under the influence of Component B's degraded condition.

Assuming Component A's vibration amplitude is $V_A(t)$, vibration signals are often the superposition of multiple excitation factors, exhibiting substantial uncertainty and constituting a random process. To simplify the model and facilitate subsequent simulation calculations, we denote $v_A(t)$ as follows:

$$v_A(t) = v_0 + \gamma \cdot (\tau_A(t) - t_A) \tag{3}$$

where v_0 is the baseline vibration level, $\gamma > 0$ is the sensitivity coefficient, and t_A is the actual operating time of component A. $\tau_A(t) - t_A$ can be understood as additional damage caused by coupling between components, which makes component A more prone to deterioration and requires more frequent maintenance.

It should be noted that the vibration model has been simplified to a linear deterministic function to capture the dominant upward trend that emerges as the equipment ages; meanwhile, the inherent stochastic degradation of Component B is described entirely by a gamma process. This balance ensures the physical plausibility and computational efficiency of real-time rolling life-time optimization without compromising the validity of the coupling mechanism or maintenance decisions. The core research objective of this study is to design dynamic grouping maintenance strategies and rolling-horizon optimization schemes for heterogeneous coupled systems, rather than to develop or benchmark different vibration and degradation model structures. The current modeling form is selected as a physically interpretable and computationally tractable baseline, which can effectively capture the main monotonic degradation and saturating coupling characteristics within the normal lifecycle.

$g(D_B(t))$ is coupling function for component B with respect to component A. Regarding the application of coupling functions [38-42], various methods have been proposed to model dependencies between components, such as copula functions, joint stochastic processes, acceleration models, multi-stress coupling, or dynamic coupling. We formulate the coupling function as follows:

$$g(D_B(t)) = 1 + \delta_{AB}\frac{D_B(t)}{1+D_B(t)} \tag{4}$$

The coupling coefficient between component B and component A is denoted as $\delta_{AB} > 0$, and the degradation level of component B, $D_B(t)$, affects the failure rate of component A in a nonlinear manner. As the degradation level of component B increases, the degradation factor $g(D_B(t))$ gradually grows, leading to greater excess damage to component A. We selected this form of coupling function based on the following two considerations:

(1) Bounded acceleration effect: This function increases monotonically with the degradation of the coupled components $D_B(t)$, while remaining bounded. This reflects physical reality: interactions between components accelerate degradation, but cannot grow indefinitely. Many electromechanical systems exhibit

this saturating behavior due to design constraints, load limitations, or material properties.

(2) Consistency with existing literature: In multi-component maintenance research, similar bounded or fractional forms are commonly used to model the interaction effects between components. For example, Wildeman and Dekker [1,2] used bounded interaction factors to represent economic and mechanical dependencies between components. These forms provide an intuitive and physically reasonable approach that captures the impact of one component's degradation on another without overestimating the effect.

This coupling function is bounded, monotonically increasing, and asymptotically stable, which conforms to the physical law of degradation acceleration. It is not arbitrarily selected and has clear mathematical rationality.

Therefore, the failure of Component A is described by an equivalent age $\tau_A(t)$ Weibull distribution, with its reliability function and failure rate given by:

$$R_A(\tau_A) = exp\left[-(\frac{\tau_A}{\eta_A})^{m_A}\right], \lambda_A(\tau_A) = \frac{m_A}{\eta_A}(\frac{\tau_A}{\eta_A})^{m_A-1} \tag{5}$$

3.1.2. Failure model for component B

The degradation state of Component B is influenced by the vibration amplitude of Component A, thus exhibiting less pronounced standard fixed-parameter gamma degradation. Therefore, refer to [43], we modify the shape parameter of the gamma process from a constant to a linear function of another degradation process:

$$\alpha_B(t) = \alpha_B + \delta_{BA} \cdot v_A(t) \tag{6}$$

where $\alpha_B > 1$ is the intrinsic shape parameter of component B, and $\delta_{BA} > 0$ is the coupling coefficient of component A with respect to component B. Therefore, the degradation process of component B follows a non-homogeneous gamma process with parameters varying over time, namely:

$$D_B(t) \sim \Gamma(\tilde{\alpha}_B(t), \beta_B), \tilde{\alpha}_B(t) = \int_0^t \alpha_B(s)\, ds \tag{7}$$

among them $\tilde{\alpha}_B(t)$ is the cumulative shape parameter. From the properties of the gamma process, the expected trajectory of the degradation quantity is:

$$E[D_B(t)] = \mu_B(t) = \frac{\tilde{\alpha}_B(t)}{\beta_B} = \frac{1}{\beta_B}\int_0^t \alpha_B(s)\, ds \tag{8}$$

The Gamma process is a classical and effective model for describing the continuous and monotonic degradation process of electronic components, which is consistent with the degradation trend shown in Fig. 7.

3.1.3. Properties of the coupling model

To describe the dependency relationships between heterogeneous components, we have established a mathematical model by introducing concepts such as coupling functions, equivalent age, and acceleration factors. This section discusses the model's nonlinear characteristics, stability, and mathematical properties; the existence of optimal solutions will be addressed in Section 3.4.2 below.

(1) Nonlinearity Analysis

The coupling function $g(D_B(t)) = 1 + \delta_{AB}\frac{D_B(t)}{1+D_B(t)}$ is a typical fractional nonlinear function, which can describe the nonlinear acceleration effect of Component B's degradation on Component A's equivalent age. This nonlinear form ensures that the acceleration effect grows with degradation but remains bounded, which is consistent with the physical laws of electromechanical systems.

The equivalent age of Component A is defined as the integral of the nonlinear coupling function over time, which forms a nonlinear cumulative damage model. The equivalent age does not increase linearly with service time, but is affected by the real-time degradation state of Component B, forming a closed-loop nonlinear coupling.

The shape parameter of Component B's Gamma process is a linear function of Component A's vibration amplitude, which is in turn affected by Component A's equivalent age. This forms a bidirectional closed-loop nonlinear coupling between the two components, where the degradation state of each component dynamically affects the degradation rate of the other.

(2) Stability Analysis

The stability of the model is guaranteed from two dimensions: system state evolution and algorithm iteration:

The coupling function adopted in the model is strictly bounded:$1 \le g(D_B(t)) \le 1 + \delta_{AB}$, and the vibration amplitude model also has a bounded growth rate. This ensures that the degradation acceleration effect of the bidirectional coupling will not diverge infinitely, and the degradation state of both components will not exceed the failure threshold prematurely under normal operation. The system state evolution is stable within the preset design life cycle.

3.2. Group maintenance optimization model

Based on established physical models and component-specific maintenance strategies, an optimization model is developed to minimize both the long-term cost rate and unavailability of the system. This model simultaneously accounts for the impact of proactive maintenance and maintenance resources on maintenance activities.

3.2.1. Setting maintenance thresholds

(1) Failure Thresholds

Let T_A^c,D_B^c, denote the failure thresholds of components A and B, respectively. Component failure thresholds are typically specified during system design or testing phases and are not treated as optimization variables. Therefore, this paper treats them as constants.

(2) Preventive Maintenance Thresholds

The degradation process of Component B is influenced by the vibration amplitude of Component A. Its shape parameter expands into a time-varying function as shown in Eq. (6). According to Eq. (8), under a given failure threshold D_B^c, solution $t_B^F$for Condition$\mu_B(t_B^F) = D_B^c$can be approximated as the failure time of Component B under coupled conditions. For setting the preventive maintenance threshold, this paper adopts a proportional approach:

$$T_A^p = \alpha_A^p T_A^c, D_B^p = \alpha_B^p D_B^c \tag{9}$$

where represents the discount factor, which controls the optimization range of preventive maintenance while directly reflecting its conservatism level. A smaller value indicates more risk preference, while a larger value signifies higher utilization of service life but increased failure risk.

(3) Group Maintenance Threshold

To describe how to perform opportunistic group maintenance, a group maintenance threshold is introduced. When a component approaches its preventive maintenance threshold and another component is also due for maintenance, simultaneous maintenance of both components is considered to share setup costs. Therefore, this paper sets the group maintenance threshold as a proportional model based on proximity to the preventive maintenance threshold:

$$T_A^o = \beta_A^o T_A^p, D_B^o = \beta_B^o D_B^p \tag{10}$$

where $\beta_A^o, \beta_B^o \in (0.7,0.9)$ represents the discount factor that controls the optimization interval for group maintenance. When component A reache $t_A \in \left[T_A^o, T_A^p\right]$ and component B requires preventive or corrective maintenance, this triggers opportunistic group maintenance for component A, the same applies to component B.

3.2.2. Definition of decision variables

The decision variables are defined as the preventive maintenance threshold discount factor and the grouped maintenance threshold discount factor $\{\alpha_A^p, \alpha_B^p, \beta_A^o, \beta_B^o\} \in (0.7,0.9)$ for components. These four variables are selected as the core decision variables because they directly map to all maintenance thresholds of the system, and can fully control the maintenance strategy while avoiding the dimension explosion of the decision space, which is a common and effective setting in maintenance optimization research. The failure threshold, preventive maintenance threshold, and grouped maintenance threshold of a component collectively from the threshold vector $\Theta = (T_A^o, D_B^o, T_A^p, D_B^p, T_A^c, D_B^c)$. A maintenance action sequence $Z = (x_{A,k}, x_{B,k}, y_{A,k}, y_{B,k}, u_k)$ is generated based on the threshold vector.

Maintenance decisions for Component B are based on its degradation state, which is continuous at the physical level. In practical maintenance activities, a series of thresholds are typically set to discretize the degradation process, such as the DSSD and two-dimensional strategy map methods proposed in [44,45].

Define the preventive maintenance actions for the component:

$$x_{A,k} = \{0,1\}, x_{B,k} = \{0,1\} \tag{11}$$

when $t_{A,k} > T_A^p$, $D_{B,k} > D_B^p$ occurs, a value of 1 indicates preventive maintenance is being performed; otherwise, it is 0.$t_{A,k}$ represents the cumulative operating time of Component A at the kth inspection, while $D_{B,k}$ denotes the degradation level of Component B at the kth inspection.

Define corrective maintenance actions for Components A and B:

$$y_{A,k} = \{0,1\}, y_{B,k} = \{0,1\} \tag{12}$$

when $t_{A,k} > T_A^c$, $D_{B,k} > D_B^c$, a value of 1 indicates a fault requiring corrective maintenance, while 0 indicates no fault.

A method for grouped maintenance in dual-component systems [45] is provided, wherein maintenance on one component creates favorable maintenance opportunities for the other. When a component reaches age $T_A^o \leq t_{A,k} < T_A^p$ or degradation state $D_B^o \leq D_{B,k} < D_B^p$, and the other component in the system requires preventive or corrective maintenance, consider maintaining both components simultaneously to reduce costs. Note that grouped maintenance involves performing preventive or corrective maintenance on components A and B simultaneously to reduce costs. Defining grouped maintenance actions:

$$g_{A,k} = \{0,1\}, g_{B,k} = \{0,1\} \tag{13}$$

when $T_A^o \leq t_{A,k} < T_A^p$, $D_B^o \leq D_{B,k} < D_B^p$, set to 1 to indicate consideration of grouped maintenance; otherwise, set to 0. Thus, group maintenance encompasses the following scenarios:

- $x_{A,k} = 1, g_{B,k} = 1$,Component A undergoes preventive maintenance while Component B considers group maintenance.
- $x_{B,k} = 1, g_{A,k} = 1$,Component B undergoes preventive maintenance while Component A considers group maintenance.
- $y_{A,k} = 1, g_{B,k} = 1$,Component A undergoes corrective maintenance while Component B considers group maintenance.
- $y_{B,k} = 1, g_{A,k} = 1$,Component B undergoes corrective maintenance, while Component A undergoes group maintenance.
- $x_{A,k} = 1, x_{B,k} = 1$,Components A and B undergo preventive maintenance simultaneously.
- $y_{A,k} = 1, y_{B,k} = 1$,Components A and B undergo corrective maintenance simultaneously.

Assuming components undergoing early group maintenance uniformly follow preventive maintenance standards, to simplify the objective function expression, we uniformly define this as group action *u*, 1 indicates that group maintenance is performed; otherwise, 0.

$$u = \begin{cases} 1, & \begin{array}{c} if\ x_{A,k} = 1, g_{B,k} = 1\ or\ x_{B,k} = 1, g_{A,k} = 1\ or\ y_{A,k} = 1, g_{B,k} = 1 \\ or\ y_{B,k} = 1, g_{A,k} = 1\ or\ x_{A,k} = 1, x_{B,k} = 1\ or\ y_{A,k} = 1, y_{B,k} = 1 \end{array} \\ 0, & else \end{cases} \tag{14}$$

Based on the above formulation, the decision space of the model is a 4-dimensional bounded closed feasible domain ($\Omega \subset \mathbb{R}^4$), defined as:

$\Omega = \{(\alpha_A, \alpha_B, \beta_A, \beta_B) \mid 0 < \beta_i < \alpha_i < 1,\ i \in \{A, B\}\}$,Each dimension of the decision space has a clear physical meaning:

(α_A, α_B): Control the conservatism of preventive maintenance for mechanical and electronic components respectively. A smaller value means more aggressive preventive maintenance, while a larger value means higher utilization of component service life.

(β_A, β_B) : Control the opportunity window of group maintenance. A smaller value means a wider opportunity window for opportunistic maintenance, while a larger value means a stricter trigger condition for group maintenance.

The constraint ($0 < \beta_i < \alpha_i < 1$) ensures that the group maintenance threshold is always lower than the preventive maintenance threshold, which avoids logical conflicts in maintenance decisions. The Pareto optimal solutions obtained by NSGA-II are all located within this feasible domain, and their distribution characteristics reflect the trade-off relationship between decision variables and optimization objectives.

The dynamic group maintenance logic adopted in this paper follows the classical grouping paradigm for multi-component systems, and defines clear triggering criteria based on degradation state and maintenance threshold. The grouping mechanism comprehensively considers economic dependence, residual life waste constraint and maintenance resource limitation, and standardizes the judgment order of preventive and corrective maintenance actions. Appropriate logical simplification is conducted to focus on the core bidirectional coupling degradation and rolling optimization analysis, while retaining all essential engineering connotation and constraint rules required for group maintenance decision-making.

3.2.3. Maintenance costs

(1) Individual Component Maintenance

Performing preventive replacement individually incurs preventive costs. Generally, the preventive cost for component (denoted as C_i^p) can be divided into two parts [46]:

$$C_i^p = c_i^p + c_d \cdot d_i^p \tag{15}$$

among these, $c_d \cdot d_i$ represents downtime costs due to production losses during replacement, preventive maintenance requires d_i^p time units, and c_i^p encompasses all other component costs (spare parts, labor, setup).

Similarly, the corrective replacement cost for component i is:

$$C_i^c = c_i^c + c_d \cdot d_i^c \tag{16}$$

where $i \in \{A, B\}$ and c_d represent the system downtime cost rate per unit time, while d_i^p, d_i^c denotes the maintenance time for performing preventive or corrective maintenance on components. For preventive component replacement, we refer to replacement before component failure. For corrective component replacement, we refer to replacement upon component failure. Additionally, a fixed inspection cost $C_{ins} = C_{ins,A} + C_{ins,B}$ is incurred each time a component is inspected.

(2) Group Maintenance Savings

It is important to note that when maintenance activities occur simultaneously, setup costs can be shared [7,46]. We define the cost of group maintenance savings as:

$$C_G = a \cdot (c_A + c_B) + b \cdot (d_A + d_B) \cdot c_d \tag{17}$$

where $c_A = x_{A,k}c_A^p + y_{A,k}c_A^c$, $c_B = x_{B,k}c_B^p + y_{B,k}c_B^c$ represent the individual maintenance costs of components, $a(0 < a < 1)$ denotes the cost savings factor for joint maintenance, $d_A = x_{A,k}d_A^p + y_{A,k}d_A^c$, $d_B = x_{B,k}d_B^p + y_{B,k}d_B^c$ denote the maintenance duration for individual components, and represents the time savings factor for joint maintenance. Based on the study of system economic dependency in [2], we set the cost savings factor to 15% of the total maintenance cost per component, i.e., $a = 0.15$, and the time savings factor to 20% of the original total maintenance duration, i.e., $b = 0.2$. It should be clarified that grouped maintenance cost savings represent the expenses saved through joint maintenance, not the total cost of grouped maintenance.

(3) Penalty Costs

The penalty function is designed to constrain the negative effects of improper group maintenance, which includes two core terms: lifespan wastage penalty and resource shortage penalty. This design is consistent with the classic framework of dynamic group maintenance optimization. The lifespan wastage penalty avoids the loss of component service life caused by excessive premature opportunistic maintenance, while the resource shortage penalty quantifies the additional cost of maintenance resource overload during simultaneous multi-component maintenance. The two terms together balance the cost-saving benefits and potential risks of group maintenance. As previously stated, penalty costs comprise two components:

Lifespan wastage costs due to premature maintenance: To describe this lifespan wastage caused by "premature maintenance", Zeng et al. [26] introduced the concept of "waste residual." This study adopts the relative lifespan wastage measure:

$$W_{A,k} = \left(\frac{T_A^p - t_{A,k}}{T_A^p}\right)^+, (x)^+ = max(x, 0) \tag{18}$$

where $t_{A,k}$ represents the state of Component A at the kth inspection point. When group maintenance is considered during the kth inspection (i.e. $g_A = 1$) and $T_A^o < t_{A,k} < T_A^p$, $W_{A,k} > 0$ indicate the presence of life loss.

Similarly, the relative life loss of Component B can be defined as:

$$W_{B,k} = \left(\frac{D_B^p - D_{B,k}}{D_A^p}\right)^+ \tag{19}$$

Therefore, the penalty cost incurred due to wasted lifespan caused by group maintenance is:

$$C_k^w = c_A^w W_{A,k} g_A + c_B^w W_{B,k} g_B \tag{20}$$

among these, $c_A^w, c_B^w > 0$ represents the unit penalty coefficient.

Penalty Costs from insufficient maintenance resources: In actual maintenance activities, resource constraints are rarely hard limits. When resources fall short, organizations often overdraw resources through overtime work or emergency mobilization, incurring additional costs. Therefore, this paper introduces resource constraints into the model as penalty terms. Assuming various types of maintenance resources are uniformly described as maintenance resource capacity R, R_{max} denotes the upper limit of maintenance resource capacity. Preventive and corrective maintenance consume different resource quantities. The resource demand at the kth inspection is defined as:

$$R_k = \sum_{i \in \{A,B\}} [r_i^p (x_{i,k} + g_{i,k}) + r_i^c y_{i,k}] \tag{21}$$

where r_i^p , r_i^c represent the resource requirements for performing preventive or corrective maintenance on component i. When $R_k > R_{max}$ occurs, a resource shortage arises, and the resource shortage amount is:

$$\psi_k = (R_k - R_{max})^+ \tag{22}$$

The penalty for insufficient resources during the kth inspection is:

$$C_k^r = c_r \cdot \psi_k \tag{23}$$

among these, c_r is the penalty coefficient. The resource model in this paper adopts a penalty-based framework to describe the resource constraints in maintenance activities, which is consistent with the common treatment in maintenance optimization research. The model can be extended to a more detailed dynamic resource allocation model in future work. The deterministic cost model is adopted as a basic simplification to focus on the core mechanism of bidirectional coupling and dynamic maintenance grouping. In practical engineering, maintenance costs may have random uncertainty, which will be further considered in the extended model.

The penalty coefficients are determined based on the typical value range of maintenance engineering and the parameter settings in relevant research, rather than purely empirical selection. The selected values can effectively balance the grouping benefits and penalty risks, and their rationality is further verified by sensitivity analysis.

3.2.4. Objective function and constraints

The optimization objectives of this paper are set as the minimization of long-term system cost rate and system unavailability, which are the core and most widely recognized metrics in maintenance optimization research. The long-term cost rate fully quantifies the total economic input of maintenance activities, covering preventive maintenance cost, corrective maintenance cost, downtime loss, inspection cost, and penalty cost for improper grouping. System unavailability directly reflects the reliability performance of the serial system, which is the key indicator for industrial operation management. The dual-objective framework can balance the inherent trade-off between economy and reliability in maintenance decisions, which is more suitable for practical engineering scenarios than single-objective optimization. On the basis of the standard objective function form, we further introduce penalty terms for lifespan wastage and resource shortage, and combine the bidirectional coupling degradation mechanism of heterogeneous components, making the objective function fully adapted to the dynamic group maintenance scenario of this study.

The system has a finite lifetime $T_S \in [0,T]$, with periodic inspections conducted at intervals of $\tau = T/K$, K denotes the number of inspections. During the *k*th inspection, the preventive maintenance threshold, failure threshold, and group maintenance threshold are calculated based on the optimized discount factor, enabling the determination of the corresponding maintenance action sequence $Z = (x_{A,k}, x_{B,k}, y_{A,k}, y_{B,k}, u_k)$. The corresponding cost model is presented in Section 3.2.2. Under maintenance action sequence $Z = (x_{A,k}, x_{B,k}, y_{A,k}, y_{B,k}, u_k)$, the total maintenance cost within the system's finite lifetime [0, T] is:

$$C_{tot}(0,T) = \sum_{k=1}^{k}[(C_A^p \cdot x_{A,k} + C_B^p \cdot x_{B,k} + C_A^c \cdot x_{A,k} + C_B^c \cdot x_{B,k} + C_{ins}) - C_G \cdot u_k + C_k^w + C_k^r] \quad (24)$$

The corrective maintenance cost, downtime loss and penalty terms in the objective function have implicitly covered the system failure risk caused by component degradation and coupling effects. The risk of system unavailability and economic loss is quantified by the long-term cost rate and unavailability metrics. Since the failure times or degradation processes of components are random and mutually coupled, the total maintenance cost $C_{tot}(0,T)$ is a random variable. Based on the renewal process and the long-run average cost criterion [47,48], this paper employs the system's long-term cost rate, defined as:

$$J_C = \frac{1}{T} E[C_{tot}(0,T)] \quad (25)$$

The total downtime during the system planning period is $T_{down} = \sum_{k=1}^{K}(d_A + d_B)(1 - u_k b)$. Therefore, the system unavailability is:

$$J_U = E[\frac{T_{down}}{T}] \quad (26)$$

The objective function is expressed as:

$$min\,(J_C,\ J_U) \quad (27)$$

Additionally, decision variables and action sequences must satisfy the following constraints:

$$i \in \{A,B\},\ k = 1,2,\dots,K \quad (28)$$

$$0 < \tau < T \quad (29)$$

$$0 < T_A^o < T_A^p < T_A^c,\quad 0 < D_B^o < D_B^p < D_B^c \quad (30)$$

$$x_{i,k}, y_{i,k}, u_k \in \{0,1\} \quad (31)$$

$$x_{i,k} + y_{i,k} \le 1 \quad (32)$$

Eq. (28) defines the time range of the k-th inspection, ensuring all inspection and maintenance activities are carried out within the system’s finite design lifetime, in line with industrial equipment operation rules. Eq. (29) restricts the inspection interval within the system’s planned lifetime, avoiding invalid settings and ensuring the rationality of the inspection plan. Eq. (30) specifies the threshold magnitude relationship: group maintenance threshold < preventive maintenance threshold < failure threshold, to avoid excessive premature maintenance and unplanned system downtime. Eq. (31) defines maintenance action variables as binary 0-1 variables, conforming to the discrete decision characteristics of actual maintenance activities. Eq. (32) Prohibits simultaneous preventive and corrective maintenance on the same component, avoiding decision logic conflicts and complying with actual maintenance operation specifications.

3.3. Improved rolling horizon optimization method

When formulating dynamic maintenance optimization strategies, the rolling horizon optimization (RHO) method has been widely adopted in existing research [20, 49-51]. However, standard RHO frameworks are mostly based on independent component degradation assumptions and fixed maintenance thresholds, which cannot be directly applied to the bidirectionally coupled heterogeneous system in this study. Therefore, we propose an improved rolling time-domain optimization framework, which includes:

(1) Integrate the bidirectional closed-loop coupling degradation model into the RHO framework, and update the real-time coupling-affected degradation state of components in each prediction window;

(2) Embed the dynamic group maintenance decision mechanism with lifespan wastage and resource shortage penalties, and synchronously optimize the group maintenance thresholds in each rolling step;

(3) Nest the NSGA-II bi-objective optimization algorithm to realize the balanced optimization of cost rate and unavailability in each finite prediction window.

This improved framework evaluates the overall performance of the system using long-term cost rate and unavailability, and achieves global optimization by solving for local optima in each rolling window.

3.3.1. Local optimization model

Within this window, the failure and degradation states of the component are obtained based on the coupled physical degradation model described in Section 3.1. Using threshold vector, a local optimization model is constructed:

$$min\left(J_{C,RH},\ J_{U,RH}\right) \tag{33}$$

among these, $J_{C,_{RH}} = \frac{1}{H}E[C_{tot}(t_k, t_k + H)]$ represents the cost rate within the forecast window $[t_k, t_k + H]$, and $J_{U,RH} = E[T_{down,RH}/H]$ denotes the unavailability within the forecast window. The values of the group maintenance threshold, preventive maintenance threshold, and corrective maintenance threshold satisfy:

$$0 < T_A^o < T_A^p < T_A^c, 0 < D_B^o < D_B^p < D_B^c \tag{34}$$

Within the rolling time-domain framework, the predicted specific maintenance actions are implemented only at the current decision moment. When the system evolves to the next decision moment t_{k+1}, the state X_{k+1} is updated, and a new local optimization problem is reconstructed and solved. This “predict-optimize-roll-update” approach dynamically adjusts preventive maintenance thresholds and actions using real-time degradation information. Simultaneously, by incorporating premature replacement and resource overload impacts directly into the cost function through lifetime wastage penalties and resource shortage penalties, it achieves more economically viable and implementable maintenance decisions over long-term operation.

3.3.2. Predictive window configuration

Within the rolling time-domain framework, the length of the predictive window is a critical parameter determining effectiveness. A window that is too short tends to focus solely on the current or next cycle, overlooking mid-term maintenance opportunities. Conversely, an excessively long window, while theoretically beneficial for long-term gains, increases forecasting difficulty and reduces accuracy. [3,4,7,10] suggest that the window size must ensure all components undergo at least one preventive maintenance cycle. This paper sets H as an integer multiple of the inspection cycle, i.e., $H = N\tau$, where N reflects the number of inspections within the predictive window.

In subsequent simulation experiments, the prediction window length is set to $N = 15$ (15 inspection cycles), with sufficient theoretical, literature, and simulation verification basis:

(1) According to the classic conclusions of multi-component maintenance optimization, the window size must ensure that all components undergo at least one preventive maintenance cycle within the window. The MTBF of Component A is 10.5 time units, and the average failure time of Component B is about 12 time units under coupling conditions. The selected fully covers the preventive maintenance cycle of both heterogeneous components, which meets the core requirement of RHO

for maintenance optimization.

(2) The 15-cycle window setting achieves the optimal balance between prediction accuracy and computational efficiency. It avoids the short-sightedness of short windows and the high uncertainty and computational complexity of long windows, and is fully compatible with the iterative calculation of the NSGA-II algorithm in each rolling step.

(3) We compare the comprehensive performance of the strategy under different window sizes (5, 10, 15, 20, 25 inspection cycles). The results show that when $N = 15$, the system achieves the optimal trade-off between long-term cost rate and unavailability, with the lowest comprehensive operation cost and the highest reliability performance. For specific results, see Section 4.6, Parameter Sensitivity Analysis.

3.4. Rolling time domain method based on NSGA-II

In Section 3.2, the maintenance problem for a two-component system composed of heterogeneous components is formulated as a finite-period dual-objective optimization model under specified inspection intervals and failure thresholds. Combined with the rolling time-domain approach, the maintenance problem for each window $[t_k, t_k + H]$ can be formulated as follows: Given the current system state, optimize locally to minimize the cost rate and unavailability within the window to obtain a discount factor, then compute the maintenance threshold to generate maintenance actions. Due to the inherent trade-off between cost and availability, single-objective weighted sum methods may overlook efficient solutions on non-convex Pareto fronts. To obtain a set of non-dominated compromise solutions, this study employs NSGA-II for solving the dual-objective problem, a method also used in references [5,23]. NSGA-II is selected because it is the most widely used and representative algorithm for bi-objective maintenance optimization problems. It can effectively provide well-distributed and convergent Pareto solutions, which is suitable for the proposed rolling horizon framework.

3.4.1. Algorithm flowchart

For this purpose, this paper proposes a rolling time domain method based on NSGA-II. The outer rolling time domain continuously updates the prediction window and status during system operation, while the inner NSGA-II multi-objective genetic algorithm optimizes the discount factor at each inspection time point. This yields a maintenance threshold within the window that balances economic and unavailability metrics, thereby determining the current decision.

Step 1 Initialization Phase: Set the initial states of components A and B according to the model specifications, while simultaneously configuring other parameters required by the model and the NSGA-II algorithm.

Step 2: Window Construction and Chromosome Encoding: At the current decision moment t_k, observe and update the system state, then construct the prediction window $[t_k, t_k + H]$, the initial population is $P = \{g_1, g_2, \ldots, g_k\}$. Within this window, the discount factors for preventive maintenance and group maintenance thresholds serve as decision variables. These are encoded as real numbers and sequentially arranged to form a chromosome $g_k = [\alpha_A^p, \beta_A^o, \alpha_B^p, \beta_B^o]$, as shown in Fig. 3. This chromosome represents a set of threshold discount factor combinations used within Window $[t_k, t_k + H]$ to drive maintenance decisions and simulation evaluations within the window.

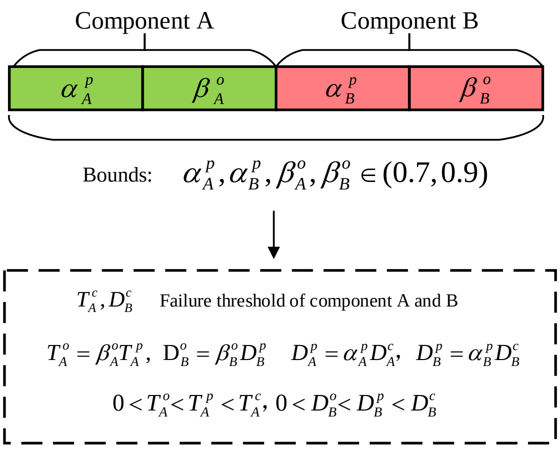

Figure 3. Schematic diagram of chromosome coding.

Step 3: Fitness Calculation: For each chromosome within the prediction window, simulate the failure and degradation processes of components based on the degradation model in Section 3.1. Advance system evolution within the window according to inspection time points, and execute corresponding maintenance actions when maintenance conditions are triggered based on the optimization model in Section 3.2. After maintenance, reset the state according to model rules and accumulate maintenance costs and downtime. Calculate the cost rate and unavailability within the window according to Section

3.3.1 to obtain the objective vector corresponding to this chromosome:

$$f(g_k) = \left(f_1(g_k), f_2(g_k)\right) \tag{35}$$

Among these, $f_1(g_k)$ represents the cost rate, and $f_2(g_k)$ denotes the unavailability.

Step 4: Non-Dominating Sorting and Population Evolution:

- Non-Dominating Sorting: Merge the parent generation P and offspring generation Q to obtain $R = P \cup Q$. Perform fast non-dominating sorting to derive distinct non-dominating layers and assign each individual a non-dominating rank.
- Crowding Distance: Calculate the crowding distance within each non-dominating layer to measure the sparsity of individual distribution in the objective space.
- Selection Operator: Employ tournament selection based on rank and crowd distance, prioritizing individuals with lower rank. When ranks are equal, select the individual with greater crowd distance.
- Crossover Operator: Apply simulated binary crossover (SBX) for real-valued encoding to the selected parents, generating offspring.
- Mutation Operator: Each gene position in a chromosome undergoes polynomial mutation with a fixed mutation probability.
- Repair Operator: To ensure individuals consistently satisfy the physical constraints of variable boundaries and thresholds, the algorithm performs constraint processing on each offspring chromosome after crossover and mutation: First, real-valued genes undergo boundary clipping to fall within preset ranges, subsequently, maintenance thresholds for each component are computed via discount factors through threshold mapping relationships, and strict inequality constraints are applied to satisfy threshold magnitude relationships.
- Elite Retention and Update: Employing an NSGA-II elite strategy, the parent and offspring generations are merged and filled sequentially by non-dominated layers to form the next generation. When the final layer exceeds the population capacity, truncation occurs based on decreasing crowding distance until the preset population size is achieved. This process repeats until the maximum iteration count is reached or successive generations show insufficient improvement on the Pareto front.

Step 5: Execute Current Decision and Update Rollup: Based on the Pareto non-dominated solution set obtained in the current window, establish the following decision preference rule to select the discount factor for generating maintenance actions. Let $G = \{g_1, g_2, \dots, g_i\}$ denote the Pareto non-dominated solution set, with $f_1(i)$ and $f_2(i)$ representing the cost rate and unavailability rate of solution g_i, respectively.

- Normalization to place both target values on the same scale. Apply minimum-maximum normalization to each target:

$$n_1(i) = \frac{f_1(i) - min(f_1)}{max(f_1) - min(f_1)}, n_2(i) = \frac{f_2(i) - min(f_2)}{max(f_2) - min(f_2)} \tag{36}$$

Among these, $min(f_1)$ and $max(f_1)$ represent the minimum and maximum values of f_1 across all solutions, respectively, and f_2 follows the same principle.

- Using weighted preferences, the weights for optimal solution selection are set based on the actual operation requirements of electromechanical systems. In the conventional operation stage, equal baseline weights are adopted for the cost rate and unavailability objectives to achieve a balanced trade-off between economy and reliability. In the urgent task stage, the weight of unavailability can be dynamically increased to prioritize system reliability. This dynamic weight setting is a common and reasonable practice in multi-objective maintenance optimization, ensuring the engineering applicability of the decision-making mechanism.

In this paper, we set weights and, with the selection criteria being:

$$s_{best} = arg\min_i(w_{cost} \cdot n_1(i) + w_{unavailability} \cdot n_2(i)) \tag{37}$$

Among these, ensure $w_{cost} + w_{unavailability} = 1$. After selecting the optimal solution, execute the maintenance action at the current time to update the system state. Then roll forward until the planned lifetime is reached. The algorithm flowchart is shown in Fig. 4.

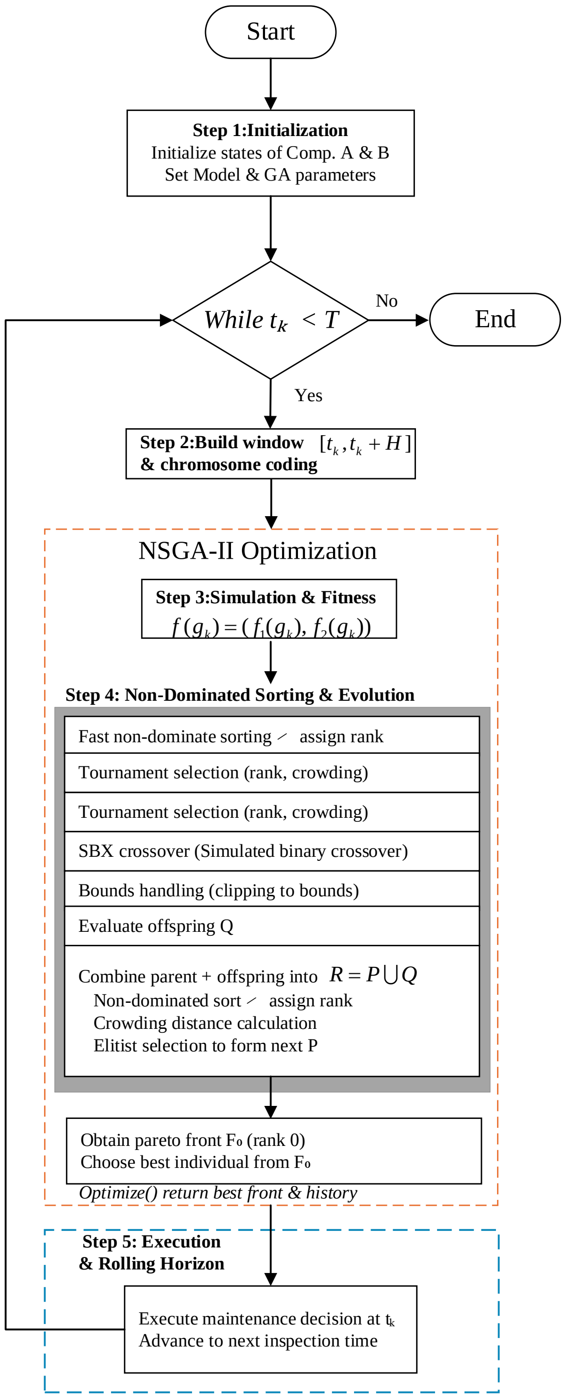

Figure 4. Algorithm flowchart.

3.4.2. Analysis of computational complexity and existence of optimal solutions

The computational complexity of the proposed algorithm is determined by the population size, maximum iteration number, and the number of decision variables. The complexity level is acceptable for engineering applications, which is consistent with general multi-objective evolutionary algorithms for maintenance optimization. The hyperparameters including population size, iteration number, crossover probability, and mutation probability are set according to classical empirical values in relevant literature, ensuring the effectiveness and stability of the algorithm. The convergence of the algorithm is guaranteed by the non-dominated sorting, crowding distance calculation, and elite retention strategy. The rolling horizon mechanism with finite window further ensures the stability and convergence of the whole optimization process.

Based on the nonlinearity and stability analysis in Section 3.1.3, the existence of an optimal maintenance strategy can be further guaranteed. The long-term cost rate and system unavailability constructed in this paper are continuous functions with respect to decision variables such as maintenance thresholds and grouping factors. Under the constraint of bounded degradation states and finite prediction windows, the feasible region of the optimization problem is compact and non-empty. Meanwhile, the two optimization objectives are both lower-bounded in the feasible region, satisfying the basic conditions for the existence of optimal solutions. Therefore, the Pareto optimal solution of the multi-objective maintenance optimization problem must exist in the feasible domain. This provides a solid theoretical foundation for the convergence and effectiveness of the NSGA-II algorithm, ensuring that the rolling optimization framework can obtain stable and reliable optimal maintenance decisions.

4. Numerical validation

This section employs a series of numerical simulations to validate the effectiveness of the coupled physical model and grouped maintenance optimization model proposed in Section 3. Simultaneously, three baseline strategies are formulated for comparison under identical scenarios to demonstrate the model's advanced nature. The analysis further examines the impact of coupling strength on strategy effectiveness and the influence of economic dependencies on system cost and unavailability. Component failure or degradation processes are simulated using discrete time steps as described in Section 3.1. Maintenance decisions are executed according to Section 3.2 and solved within the rolling time-domain framework based on the NSGA-II genetic algorithm outlined in Section 3.4.

4.1. Parameter settings

This paper assumes all parameters are expressed in arbitrary units, whether arbitrary cost units or arbitrary time units.

4.1.1. Component parameter settings

This section employs a series of numerical simulations to validate the effectiveness of the coupled degradation model and grouped maintenance optimization model proposed in Section 3. Given the extreme scarcity of publicly available industrial datasets that simultaneously include full lifecycle data of heterogeneous electromechanical systems with bidirectional coupling between mechanical vibration and electronic control degradation, synthetic data based on real engineering experimental parameters is adopted for numerical validation, which is a common and accepted research paradigm in maintenance optimization research. All parameters are determined according to typical engineering values and relevant literature [52,53], which are widely used in the reliability modeling of mechanical and electronic components, ensuring the numerical validation holds practical engineering significance.

In the study [52], the fitting results provided for the bearing assembly serve as representative values: $m_A = 9.6576, \eta_A = 11.0763$. Under this parameter, the mean time to failure for component A is:

$$MTTF_A = \eta_A \Gamma(1 + 1/m_A) \approx 10.5 \tag{38}$$

That is, $T_A^c = 10.5$. The degradation process of Component B is modeled as a non-homogeneous gamma process. Referring to the numerical example on coating systems in [53], this study adopts $\alpha_B = 1.2$, $\beta_B = 0.9$, with the failure threshold of Component B set as: $D_B^c = 18.5$. The life parameters and failure threshold of the component are shown in Table 2.

Table 2. Component lifespan and failure threshold parameters.

	m_A	η_A	α_B	β_B	T_A^c	D_B^c
A	9.6576	11.0763	—	—	10.5	——
B	—	—	1.2	0.9	—	18.5

The degradation rate of Component B accelerates the equivalent aging of Component A through the coupling function, with a baseline value of $\delta_{AB} = 0.6$. This means that when Component B approaches failure, the instantaneous degradation rate of Component A is amplified by a factor of 1.6, without excessively shortening Component A's failure time. Component A's vibration amplitude accelerates Component B's degradation rate. The baseline setting is $v_0 = 0.5, \gamma = 0.02$. Vibration accelerates Component B's degradation by affecting shape parameters, with a coupling coefficient of $\delta_{BA} = 0.4$.

4.1.2. Cost and maintenance resource parameter settings

Since real public datasets that include bidirectional coupling and vibration-induced degradation in heterogeneous electromechanical systems are limited, synthetic data is adopted for numerical validation, which is a common practice in maintenance optimization research. The rationality and effectiveness of the model are verified by comparative simulations. Parameters such as cost, maintenance resources, and downtime lack unified standards. This paper sets them based on engineering knowledge and preliminary experimental results, as shown in Table 3.

Table 3. Cost, maintenance resources, and downtime parameters.

	c_i^p	c_i^c	$C_{ins,i}$	r_i^p	r_i^c	d_i^p	d_i^c
A	30	60	2	2	5	0.3	0.6
B	50	100	3	4	8	0.5	1.0

Penalty costs comprise two parts: early maintenance and resource shortage. The early maintenance penalty coefficient is set to $c_A^w = 10, c_B^w = 12$, and the resource shortage penalty coefficient is set to $c_r = 20$. Assume the upper limit of available maintenance resources at each inspection time is R_{max}, and the system's downtime cost rate per unit time is $c_d = 50$.

4.1.3. Simulation parameter settings

Assuming a design life of $T = 50$, the system undergoes $K = 25$ decision points throughout the planning period, with state monitoring and maintenance decisions made at fixed inspection intervals of $\tau = 2$. The baseline detection interval in this paper is initially set to $\tau = 2$. This conservative setting is intended to ensure sufficiently frequent monitoring of the coupled degradation states of the two heterogeneous components, enabling the model to capture bidirectional acceleration effects in near real time and minimize the risk of missing critical degradation events. A systematic sensitivity analysis of the detection interval will be presented in Section 4.6.2, where parameters achieving an optimal balance between monitoring costs, state estimation accuracy, and long-term system performance will be determined. The length of the rolling time-domain prediction window is set to $N = 15$, meaning that the next 15 inspection cycles are considered in each update. This setting is intended to ensure that the rolling-time-domain framework covers at least one complete preventive maintenance cycle for both components, allowing the model to fully assess the long-term impact of maintenance decisions on cost and availability while maintaining reasonable computational efficiency. A systematic sensitivity analysis of the prediction window length will be presented in Section 4.6.3, where parameters achieving an optimal balance between decision-making myopia, computational cost, and long-term performance will be determined.

When comparing maintenance strategies, setting the number of Monte Carlo simulation repetitions to $N_{MC} = 30$ enables stable estimation of the cost rate and unavailability. For the genetic algorithm, the population size is $P = 40$, the maximum iteration count is $G_{max} = 60$, the crossover probability is 0.8, and the mutation probability is 0.1. The selection operator employs a binary tournament selection, retaining 2 elite individuals. These parameter settings reference empirical values from [54] for maintenance optimization problems and were validated in preliminary experiments to achieve a balanced trade-off between convergence speed and solution quality.

4.2. Numerical validation of the coupled degradation model

To validate the effectiveness of the proposed coupled degradation model, two scenarios were established without performing maintenance operations: coupled and uncoupled. The failure times and degradation paths of Component A and Component B were simulated respectively to observe the changes.

1. Coupled: Employing the coupled degradation model from Section 3.1 with a coupling coefficient of $\delta_{AB} = 0.6, \delta_{BA} = 0.4$. Degradation of Component B accelerates the equivalent aging of Component A, while the vibration amplitude of Component A accelerates the degradation rate of Component B.
2. No coupling: Assuming components are independent, with failure and degradation processes mutually unaffected, set $\delta_{AB} = 0, \delta_{BA} = 0$. Component A's failure time follows a standard Weibull distribution, while Component B's degradation follows a homogeneous gamma decay.

Multiple simulations demonstrate that without any maintenance interventions, the failure times and degradation paths of Component A and Component B exhibit significant differences across various scenarios. As shown in Fig. 5-8, the equivalent age and failure time distribution of Component A exhibit pronounced shifts. Under coupling conditions, both the individual sample and average degradation rates of Component B are markedly higher than those under decoupling. This demonstrates the validity of the proposed coupled degradation model.

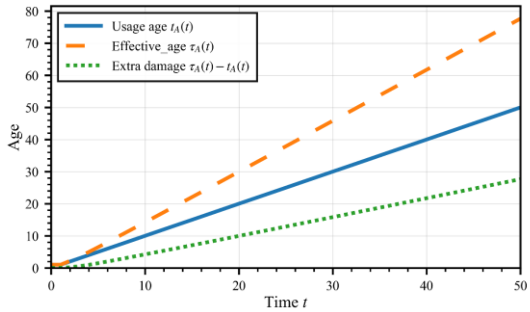

Figure 5. Evolution of equivalent age and service life under coupling of component A.

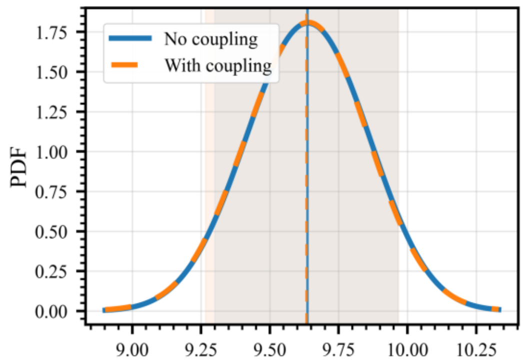

(a) Usage time

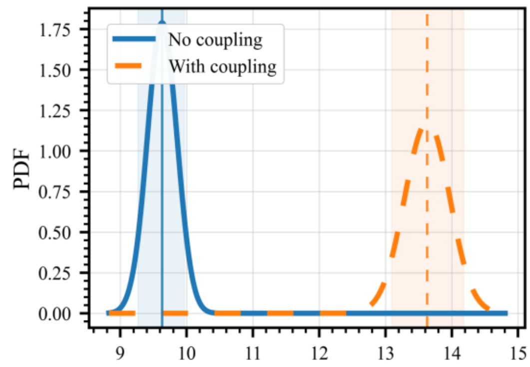

(b) Equivalent time

Figure 6. Mean time between failures distribution chart for component A.

As shown in Fig. 5, it is clearly observed that under coupled conditions, the equivalent age of Component A increases at a higher rate than its service age, and this excess loss grows increasingly larger with extended operating time. Fig. 6 displays the average distribution of Component A's failure time across two-time scales. The left panel shows that failure times measured in service age are largely overlapping under coupled and uncoupled conditions. This occurs because the study assumes that under coupling, component A's failure determination is based on service age, while equivalent age solely describes the excess damage caused by coupling. The right panel depicts equivalent age: at identical failure times, coupling yields a larger equivalent age. Consequently, a pronounced rightward shift is clearly observed under coupling, accompanied by reduced peak values and a more dispersed failure time distribution. In summary, the rightward shift and broadening of the equivalent age distribution reflect the accumulation of excess damage caused by coupling, not an alteration in Component A's usage-age failure mechanism. The degradation paths for a single sample and the average of multiple samples of Component B are shown in Fig. 7-8. It is evident that the degradation rate of Component B accelerates under coupling conditions, and the gap compared to the non-coupled scenario widens progressively.

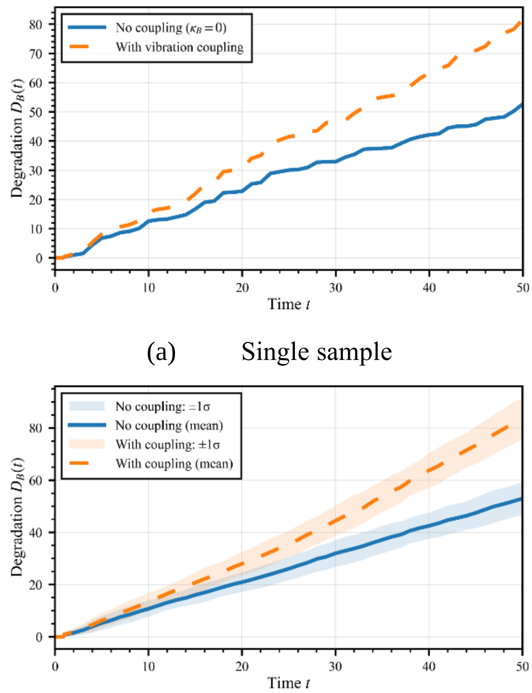

(a) Single sample

(b) Average path

Figure 7. Degradation path evolution diagram for component B.

4.3. Performance evaluation of grouping strategy and rolling time domain

This section further validates the performance of the proposed grouping strategy and rolling time domain method. For the same benchmark parameters, four comparative strategies were set. The relevant parameters of the baseline strategy are shown in Table 4.

Table 4. Maintenance thresholds for baseline strategy.

	T_A^o	D_B^o	T_A^p	D_B^p	T_A^c	D_B^c
S0	—	—	—	—	10.5	18.5
S1	—	—	8.9	15.7	10.5	18.5
S2	8.0	14.1	8.9	15.7	10.5	18.5

1. S0: Full Corrective Maintenance, i.e., corrective replacement is performed only when a component fails, with no preventive maintenance conducted.
2. S1: Static Threshold Maintenance, disregarding grouped maintenance and rolling optimization. Component A undergoes maintenance based on a fixed service life, while Component B is maintained according to a fixed degradation threshold. Maintenance decisions are not updated based on component status.
3. S2: Static Group Maintenance. Building upon Strategy 1, this introduces simple opportunistic grouping rules: when one component meets preventive or corrective maintenance conditions, if another component's age or degradation status exceeds the group maintenance threshold, both are maintained simultaneously to reduce costs.
4. S3: The rolling time domain method based on NSGA-II proposed in this paper. At each decision time, the failure time and degradation trajectory of components A/B within the prediction window from Section 3.1 are forecasted. Within the rolling time domain framework, NSGA-II is employed to optimize the discount factor, yielding maintenance thresholds for dynamic grouping maintenance. Considering resource shortage penalties and lifetime wastage penalties, only the optimal decision at the current inspection time is executed before rolling updates.

4.3.1. Optimal maintenance strategy

To identify the optimal decision variables, a sample of 300 discount factors applied to S3 was collected. The corresponding statistical data for cost rates and unavailability associated with each discount factor are presented in Table 5. Fig. 8 displays the Pareto frontier scatter plot for cost rate and unavailability under Strategy 3 using the NSGA-II algorithm. This yields the Pareto frontier and a set of Pareto non-dominated solutions. Based on decision preference rules, the discount factors selected for generating maintenance actions are: $\alpha_A^p = 0.736$, $\alpha_B^p = 0.777$ and $\beta_A^o = 0.713$, $\beta_B^o = 0.877$ corresponding to the optimal maintenance threshold of $T_A^p = 7.73$, $T_A^p = 6.0$, $D_B^p = 13.19$, $D_B^o = 11.57$.At this point, the system's long-term cost rate and unavailability are 13.4902 and 0.07074, respectively.

Table 5. Statistical data for discount factors, cost rates, and unavailability.

	N	Mean	Std	Total	Min	Medium	Max
α_A^p	300	0.78932	0.04417	236.797	0.7	0.793	0.899
α_B^p	300	0.7733	0.06334	231.99	0.7	0.7675	0.9
β_A^o	300	0.80275	0.05761	240.824	0.7	0.804	0.9
β_B^o	300	0.81072	0.06194	243.216	0.7	0.811	0.9
Cost rate	300	15.19691	0.64387	4559.07447	13.4902	15.2853	17.40003
Unavailability	300	0.07984	0.00361	23.9515	0.07064	0.07992	0.09172

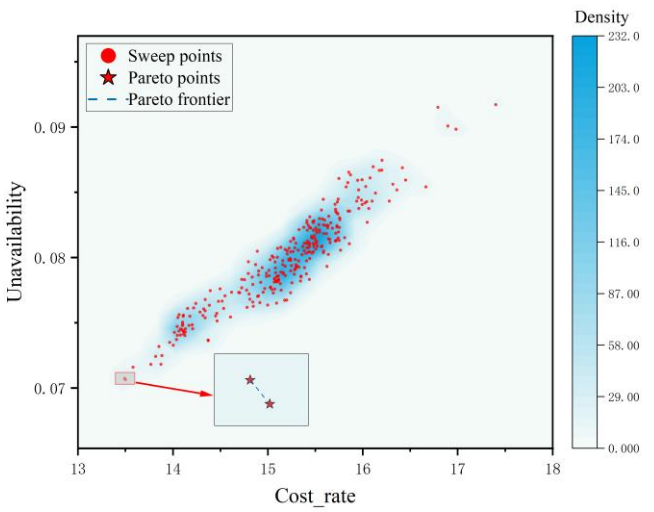

Figure 8. Cost rate and unavailability pareto scatter plot.

4.3.2. Strategy comparison

After conducting 30 Monte Carlo simulations, the results shown in Fig. 9 indicate that Strategy S3 achieves improvements over Strategy S0-2 in long-term system cost rate and unavailability of approximately 26.99%, 10.29%, and 8.93%, respectively, as well as 29.13%, 15.25%, and 12.66%, respectively.

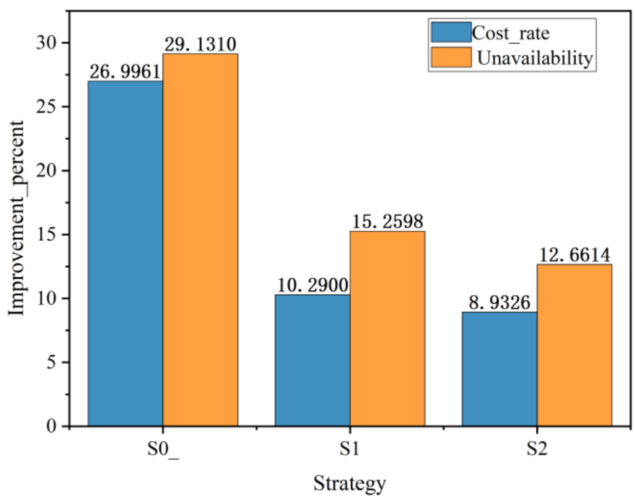

Figure 9. Comprehensive performance comparison chart.

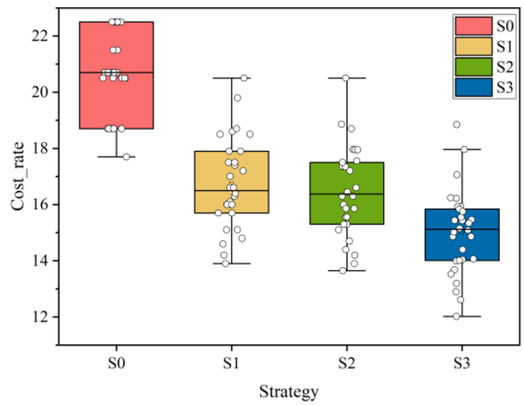

(a) Cost rate

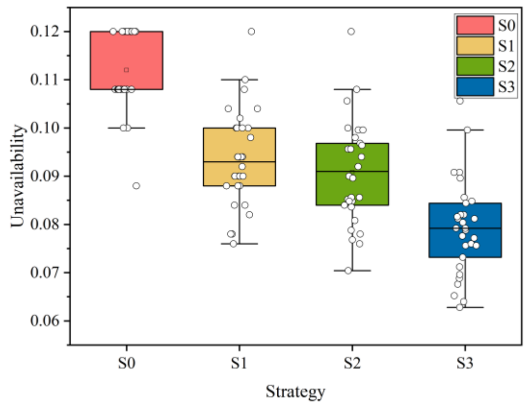

(b) Unavailability

Figure 10. Cost rate and unavailability box plot.

Fig. 10 illustrate the performance of four strategies in terms of long-term system cost rates and unavailability. The mean, standard deviation, minimum, median, and maximum values for the cost rate and unavailability of the different strategies are shown in Table 6. S0, which employs only corrective maintenance, exhibits the highest costs and unavailability. S1 and S2 introduce preventive maintenance and simple grouping rules, shifting maintenance actions toward preventive maintenance and significantly reducing both cost rates and unavailability. S3 employs intelligent algorithms within a rolling time-domain framework to dynamically adjust maintenance thresholds by optimizing discount factors, further reducing cost rates and unavailability while exhibiting smaller fluctuations and greater stability. Fig. 11 illustrates the performance of different strategies in terms of long-term system cost rates and unavailability. S0, which performs corrective maintenance, has the highest cost rates and unavailability, positioned in the upper-right corner of the figure. S1 and S2 introduce preventive maintenance and simple group maintenance respectively, reducing cost rates and unavailability to intermediate levels in the chart's middle section. S3 employs NSGA-II to dynamically adjust discount factors within a rolling time domain framework for group maintenance, further lowering cost rates and unavailability to the bottom-left quadrant of the chart.

Table 6. Mean and variance of system cost rate and unavailability.

Strategy	Cost rate					Unavailability				
	Mean	Std	Min	Med	Max	Mean	Std	Min	Med	Max
S0	20.5666	1.5297	17.7	20.7	22.5	0.112	0.0081	0.088	0.108	0.12
S1	16.7366	1.6072	13.9	16.5	20.5	0.0936	0.0100	0.076	0.093	0.12
S2	16.4871	1.5959	13.65	16.375	20.5	0.0908	0.0107	0.0704	0.091	0.12
S3	15.0144	1.5003	12.017	15.1194	18.85	0.0793	0.0098	0.0628	0.0792	0.1056

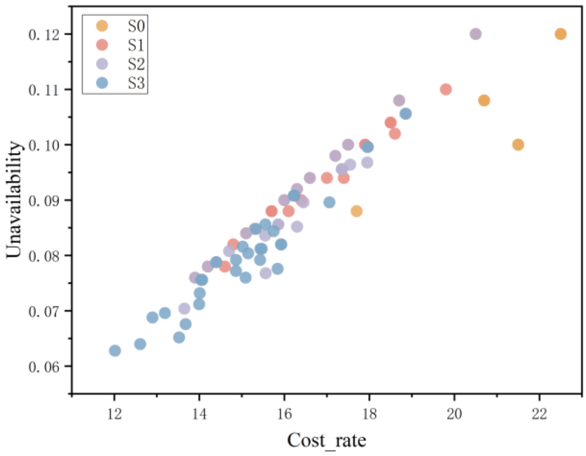

Figure 11. Performance of different strategies in cost ratio and unavailability.

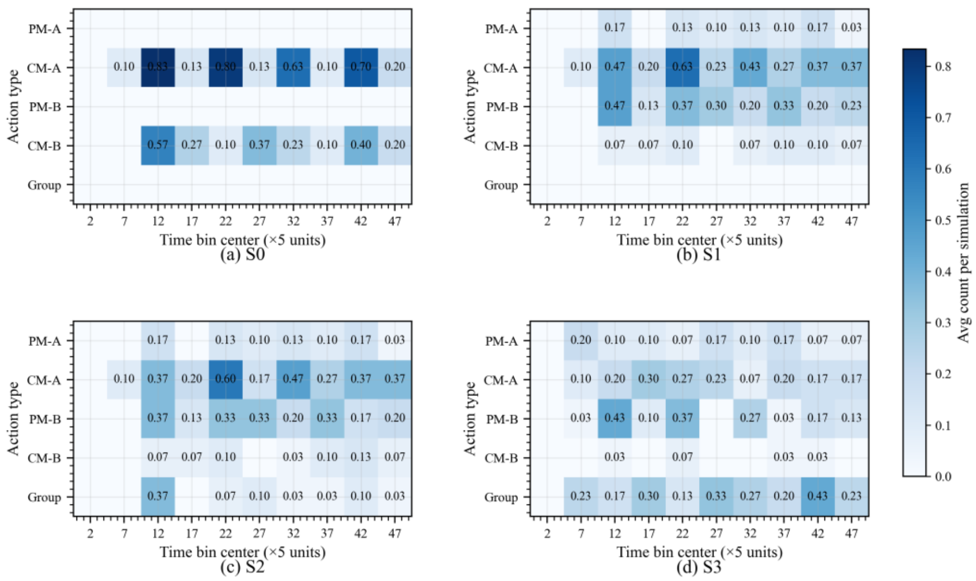

Figure 12. Heatmap of average frequency of maintenance actions across different strategies.

Fig. 12 presents a heatmap of the average frequency of maintenance actions under different strategies. The horizontal axis represents system lifetime, while the vertical axis shows various maintenance actions. The intensity of colors indicates the frequency observed across multiple simulations, illustrating differences in the types and timing of maintenance actions across different strategies. From Fig. 12, it can be observed that S0 performs only corrective maintenance—repairing components only after failure—resulting in high costs and prolonged downtime. S1 introduces preventive maintenance based on static thresholds, shifting maintenance actions toward prevention and reducing both costs and downtime. S2 implements simple grouped maintenance: when one component requires maintenance and another component meets the threshold condition, the maintenance of the second component is also considered. S3 employs dynamic grouped maintenance within a rolling time-domain framework. It continuously adjusts maintenance thresholds by optimizing discount factors using intelligent algorithms. Corrective maintenance approaches zero, while preventive maintenance and appropriately timed grouped maintenance become more frequent as component degradation accelerates. This approach achieves the lowest long-term system cost rate and unavailability.

4.4. Impact of coupling strength on strategies

We now analyze the impact of coupling strength (δ_{AB}, δ_{BA}) on different strategies by constructing four scenarios as shown in Table 7. We evaluate the performance of each strategy using two metrics: long-term system cost rate and unavailability.

Table 7. Four coupling scenarios.

Scenario	δ_{AB}	δ_{BA}
no-coupling	0	0
weak-coupling	0.3	0.2
medium-coupling	0.6	0.4
strong-coupling	1.0	0.8

Fig. 13 illustrates the performance of different strategies as coupling strength increases. Results indicate that as coupling strength increases, component degradation accelerates and maintenance actions become more frequent, leading to higher costs and increased downtime. Compared to S0-2, S3 consistently exhibits the lowest long-term cost rate and unavailability, with smaller fluctuations. This demonstrates that as coupling strength between components grows, S3's advantages also intensify.

Further comparison of strategy differences reveals: S0 performs worst across all coupling scenarios, with the most significant increases in cost rate and unavailability occurring during the transition from moderate to strong coupling. This is easily explained: as coupling intensifies, component failures become more frequent, and since S0 only performs corrective maintenance, the resulting costs and downtime are substantial. S1 and S2 exhibit intermediate performance, rising nearly in parallel with increasing coupling, with S1 slightly outperforming S2 under strong coupling. In contrast, S3 achieves the lowest cost rate and unavailability across all scenarios, with the smallest increase, demonstrating superior adaptability and robustness to coupling degradation. These results demonstrate that when systems experience significant coupling degradation, the proposed NSGA-II-based rolling time-domain method—specifically the dynamic grouping maintenance strategy (S3)—effectively mitigates coupling-induced maintenance issues, achieving a superior trade-off between cost and availability.

The stable performance improvement under different coupling strengths demonstrates the strong robustness of the proposed method. The strategy can maintain favorable performance under varying system parameters.

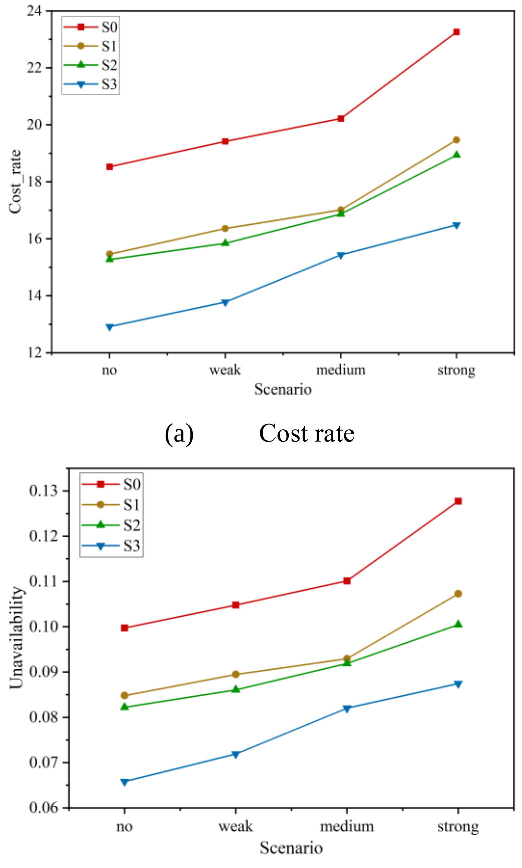

(a) Cost rate

(b) Unavailability

Figure 13. Sensitivity analysis of coupling strength.

4.5. Impact of economic dependency on system long-term cost rate and unavailability

To further understand the effect of economic dependency on grouped maintenance, we analyze the impact on cost rate and unavailability for S3, separately examining the cost-saving factor *a* and time-saving factor *b*.

4.5.1. Effect of a on system long-term cost rate and unavailability

We varied a from 0 to 20% while keeping other parameters constant to determine the minimum cost rate and unavailability for S3, with results shown in Fig. 14. The conclusion drawn is that as the cost-saving factor increases, system components become more likely to undergo maintenance together, thereby reducing the system's long-term cost rate and unavailability.

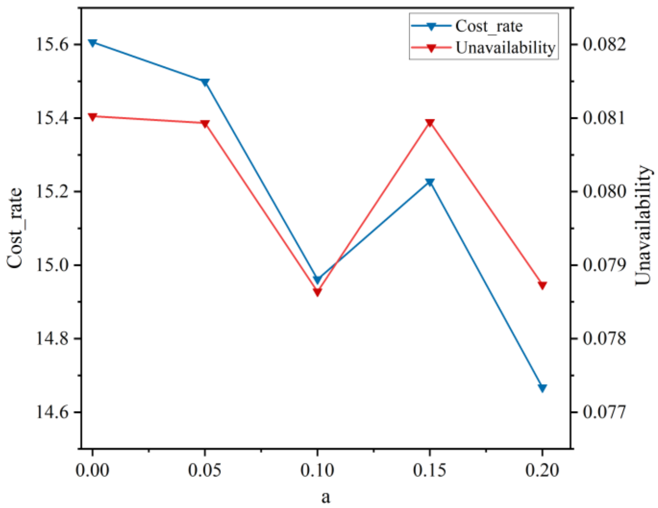

Figure 14. Impact of cost savings factor on cost rate and unavailability.

Fig. 14 indicates that as *a* increases, the cost-benefit of grouped maintenance grows, with S3 tending to maintain components together, thereby reducing the system's long-term cost rate and unavailability. To further investigate the impact of economic dependency on the system's long-term cost rate and unavailability, we considered the sensitivity of the time-saving factor *b*.

4.5.2. Effect of b on system long-term cost rate and unavailability

Similarly, by varying *b* from 0 to 50% while keeping other parameters constant, we determine the minimum cost rate and unavailability of S3. The results shown in Fig. 15 indicate that increasing the time-saving factor can significantly reduce maintenance-induced downtime and associated costs, thereby lowering system unavailability and long-term cost rates.

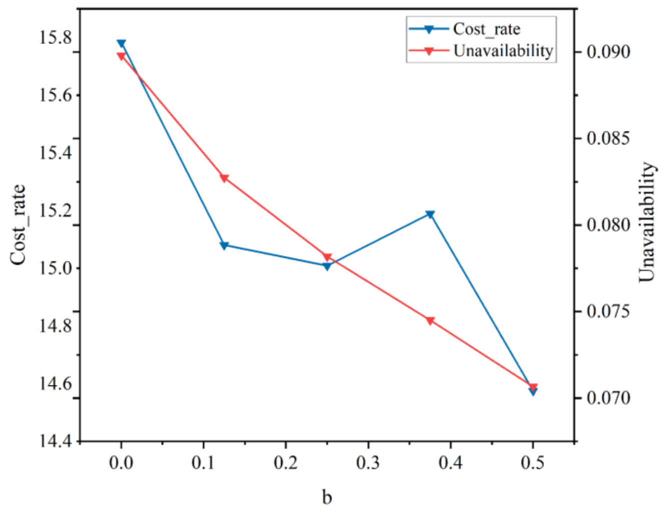

Figure 15. Impact of time savings factor on cost rate and unavailability.

Fig. 15 illustrates the impact of the time-saving factor *b* on the system's long-term cost rate and unavailability. After group maintenance, downtime is reduced by (1-*b*). Therefore, as *b* increases, maintenance-induced downtime decreases significantly, causing unavailability to decline monotonically. The system's long-term cost rate includes downtime losses and is positively correlated with downtime duration. Thus, increasing *b* not only improves availability but also drives down the cost rate by reducing downtime losses.

It is noteworthy that Fig. 14-15 show that metrics do not vary strictly monotonically with the savings factor: cost rates and unavailability may locally increase in certain intervals. This is reasonable, indicating that the penalty added to our model is effective, and the intuition that “higher savings factors always lead to greater savings” does not always hold. This occurs because when group maintenance becomes more attractive in terms of cost or time, S3 may shift toward more aggressive maintenance. For instance, increasing the frequency of batch maintenance may trigger more lifespan waste penalties. Additionally, maintaining multiple components simultaneously under constrained resources is more likely to trigger insufficient maintenance resource penalties. In these scenarios, the newly incurred maintenance penalties may temporarily outweigh the savings benefits, leading to localized non-monotonic fluctuations in cost and unavailability. Visually, S3 demonstrates rapid dynamic adjustments during local fluctuations, ensuring the system maintains low long-term cost rates and unavailability levels. This further validates the superiority of our proposed approach.

The results under different cost-saving and time-saving factors also verify the robustness and adaptability of the proposed dynamic grouping strategy.

4.6. Parameter sensitivity analysis

4.6.1. Decision variables

Based on the 300 sets of simulation sample data from Section 4.3.1, we conducted a systematic sensitivity analysis on the four core decision variables—the preventive maintenance discount factors (α_A, α_B) and the grouped maintenance discount factors (β_A, β_B) to quantify the impact of each variable on the system's long-term cost rate and unavailability, thereby verifying the model's robustness. We employed Pearson correlation analysis to quantify the strength of the linear relationship between the variables and the objectives, assessed the magnitude of the impact through standardized regression coefficients, and combined this with trend line fitting to visually illustrate the patterns of change. The core evaluation metrics included the system's long-term cost rate (mean) and system unavailability (mean); the specific results are shown in Fig. 16.

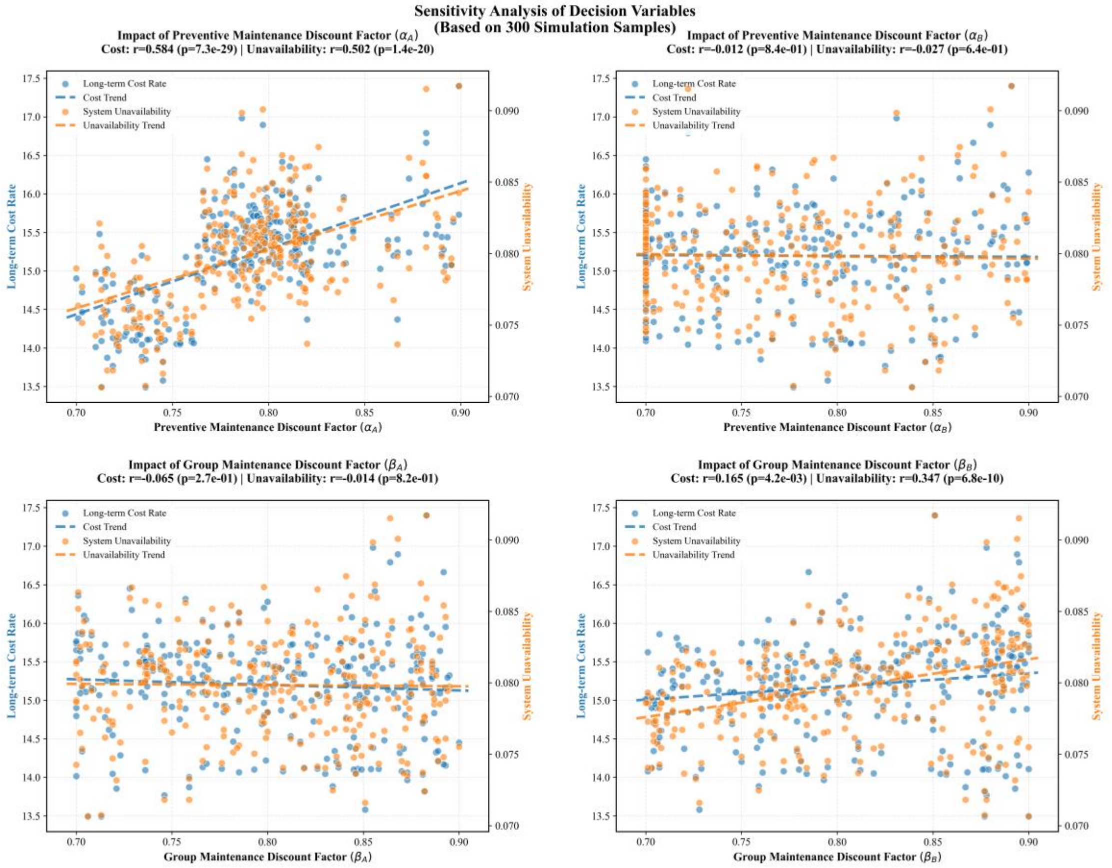

Figure 16. Sensitivity analysis of decision variables.

As shown in the top row of Fig. 16, the preventive maintenance discount factors exhibit distinct influence patterns on system performance.

For the preventive maintenance discount factor of Component A (α_A), the analysis reveals a strong positive correlation with both the cost rate ($r = 0.584, p < 10^{-28}$) and unavailability ($r = 0.502, p < 10^{-19}$). The linear trend lines indicate that increasing α_A significantly raises both metrics. This phenomenon is attributed to the fact that a higher α_A corresponds to a more conservative maintenance threshold, leading to premature preventive maintenance actions. While these actions reduce the risk of catastrophic failures, they also increase unnecessary downtime and maintenance frequency, ultimately resulting in higher long-term costs and unavailability. In contrast, the preventive maintenance discount factor of Component B (α_B) shows no significant correlation with either objective (cost rate: $r = -0.012, p = 0.838$; unavailability: $r = -0.027, p = 0.637$). The flat trend lines and low correlation coefficients indicate that variations in α_B within the tested range have negligible impact on system performance. This can be explained by the fact that Component B, as an electronic unit, exhibits a Gamma degradation process with relatively stable failure characteristics, and the system's design redundancy further mitigates the influence of its maintenance threshold fluctuations.

The bottom row of Fig. 16 presents the results for the group maintenance discount factors.

For the group maintenance discount factor of Component A (β_A), both correlation coefficients are very close to zero (cost rate: $r = -0.065, p = 0.265$; unavailability: $r = -0.014, p = 0.816$), indicating no significant impact on the system. This suggests that the opportunistic grouping strategy for Component A is robust to changes in its trigger threshold, as the preventive maintenance actions of Component A already dominate its maintenance schedule, leaving limited room for opportunistic adjustments.

Conversely, the group maintenance discount factor of Component B (β_B) shows a moderate positive correlation with unavailability ($r = 0.347, p < 10^{-9}$) and a weak positive correlation with the cost rate ($r = 0.165, p = 4.21 \times 10^{-3}$). The upward trend lines indicate that as β_B increases, both metrics rise. A higher β_B implies a stricter condition for triggering group maintenance, which reduces the opportunities for synchronizing Component B's maintenance with that of Component A. This leads to more frequent standalone maintenance actions for Component B, resulting in increased downtime and costs.

The sensitivity analysis demonstrates that the proposed model is robust to most decision variables. Only α_A has a strong impact on both objectives, while β_B has a moderate impact on unavailability. The remaining variables show no significant influence within their tested ranges. This confirms that the maintenance policy is not overly sensitive to parameter fluctuations, ensuring stable performance under varying operational conditions. Furthermore, the identified strong influence of α_A highlights its critical role in the maintenance strategy, providing guidance for parameter calibration in practical applications.

4.6.2. Inspection interval

The inspection interval is a core parameter in the condition-based maintenance framework and the rolling time-domain optimization model. Its value directly determines the frequency of monitoring system degradation and the update cycle for maintenance decisions, while also balancing inspection costs, maintenance timeliness, and long-term system performance. In this section, while keeping all other model parameters constant, we vary only the inspection interval length. We conduct single-factor sensitivity analysis for five sets of settings corresponding to 1.0, 2.0, 3.0, 4.0, and 5.0 time units, using the system's long-term cost rate and unavailability as core evaluation metrics. The analysis results are shown in Fig. 17.

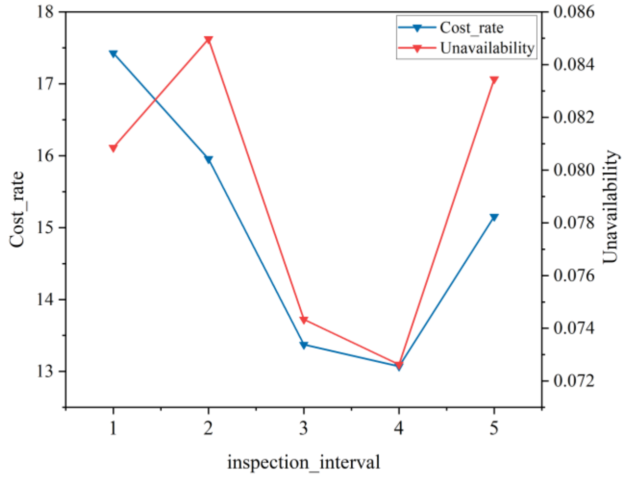

Figure 17. Sensitivity analysis of inspection intervals.

The sensitivity analysis results indicate that the inspection interval exerts a significant nonlinear influence on both the system's economic and reliability metrics. The overall trends of these two core metrics are highly consistent, exhibiting a U-shaped pattern characterized by continuous optimization followed by a significant rebound. The specific analysis is as follows:

Excessively short inspection intervals (1.0–2.0 time units): When inspection intervals fall within the range of 1.0–2.0 time units, the system's long-term cost rate remains at a high level throughout the entire interval, while unavailability shows a slight, abnormal increase. The core reason lies in the fact that while a higher inspection frequency can theoretically detect component degradation more promptly, frequent inspections result in additional downtime and inspection costs, directly driving up the system's long-term cost rate. At the same time, an overly short decision cycle triggers excessive preventive maintenance interventions, which in turn increases the frequency of unnecessary system downtime, leading to a slight rise in unavailability.

Optimal Inspection Interval Range (2.0–4.0 time units): When the inspection interval is increased from 2.0 to 4.0 time units, both core system metrics show a sustained downward trend: the long-term cost rate decreases from 15.97 to 13.08, a reduction of 18.10%; system unavailability dropped from 0.0850 to 0.0727, a decrease of 14.47%. This pattern is fully consistent with the classic theory of multi-component maintenance optimization: reasonably extending the inspection interval not only reduces the additional costs and downtime losses caused by frequent inspections but also ensures effective monitoring of the bidirectionally coupled degradation states of components, thereby avoiding unplanned failures caused by delayed condition detection; At the same time, moderate inspection intervals provide a more reasonable decision-making cycle for dynamic group maintenance, allowing for a more thorough exploitation of the cost-saving potential of opportunity maintenance and achieving simultaneous optimization of system economy and reliability.

Excessively long inspection intervals (4.0–5.0 time units): When the inspection interval exceeds 4.0 time units, both the system cost rate and unavailability experience a significant rebound: the cost rate rises from 13.08 to 15.17, an increase of 15.98%; unavailability rises from 0.0727 to 0.0835, an increase of 14.86%. The core mechanism lies in the fact that excessively long inspection intervals cause a severe lag in detecting system degradation, making it impossible to promptly capture the accelerated degradation effect caused by bidirectional coupling. This easily leads to components exceeding preventive maintenance thresholds or even experiencing unplanned post-failure, which not only significantly increases the high costs of post-failure repairs and downtime losses but also directly drives up system unavailability; At the same time, excessively long decision-making cycles also compromise the flexibility of dynamic grouping for maintenance, making it impossible to respond promptly to real-time changes in component degradation status and resulting in the loss of optimal maintenance windows.

In summary, when the inspection interval is set to 4, the system achieves the lowest costs and unavailability, striking an optimal balance between the timeliness of condition monitoring and the flexibility of maintenance decisions. This approach avoids both the additional costs and excessive maintenance associated with overly short intervals, as well as the risks of delayed condition monitoring and unplanned failures caused by overly long intervals.

4.6.3. Forecast window

To verify the impact of the prediction window length on model optimization performance within the rolling time-domain optimization framework, this section keeps all other model parameters constant and varies only the length of the prediction window. A one-factor sensitivity analysis was conducted for five sets of settings corresponding to 5, 10, 15, 20, and 25 detection cycles, using the system's long-term cost rate and unavailability as the core evaluation metrics. The analysis results are shown in Fig. 18.

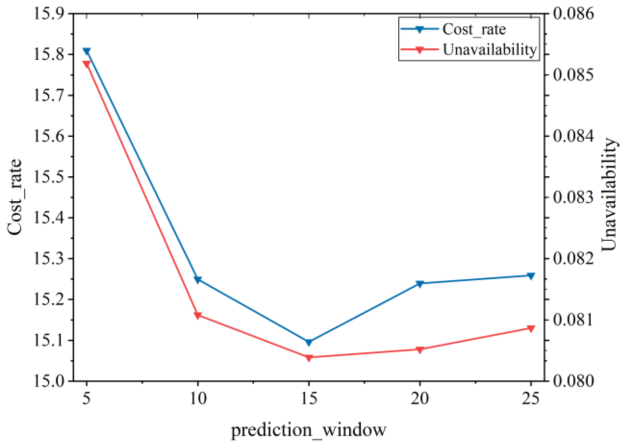

Figure 18. Sensitivity analysis of the prediction window.

The results of the sensitivity analysis show that the length of the prediction window has a significant impact on both the economic and reliability metrics of the system. The trends in these two core metrics are highly consistent, generally following a pattern of a significant initial decline followed by a slight recovery. The specific analysis is as follows:

Short window range (5–15 inspection cycles): When the prediction window is increased from 5 cycles to 15 cycles, the system's long-term cost rate decreases from 15.81 to 15.10, a reduction of 4.49%; system unavailability decreases from 0.0852 to 0.0804, a reduction of 5.63%. This pattern is fully consistent with the theoretical analysis presented earlier: an overly short prediction window leads to short-sighted optimization decisions, making it impossible to capture medium- to long-term opportunities for grouped maintenance. Consequently, it becomes difficult to share maintenance costs and reduce total system maintenance costs through opportunity-based maintenance. At the same time, frequent rolling optimization under a short window increases the number of unplanned outages, thereby driving up system unavailability.

Long-term window (15–25 detection cycles): When the prediction window exceeds 15 cycles, both core system metrics show a gradual upward trend: the cost rate rises slightly from 15.10 at 15 cycles to 15.26 at 25 cycles, and the unavailability rate rises slightly from 0.0804 to 0.0809. This is because an excessively long prediction window introduces greater uncertainty in degradation predictions, leading to a decline in the accuracy of maintenance decisions; simultaneously, an overly long planning cycle reduces the flexibility of dynamic group maintenance, making it unable to adapt to real-time changes in the system's bidirectionally coupled degradation state, ultimately resulting in a slight decline in system performance.

In summary, this paper selects 15 detection cycles as the prediction window length, achieving an optimal balance among prediction accuracy, computational efficiency, and optimization effectiveness. This approach avoids both the short-sightedness of decision-making associated with short windows and the prediction uncertainty and loss of flexibility associated with long windows. Its validity has been fully verified through the sensitivity analysis conducted in this study.

4.6.4. Penalty coefficient

To verify the robustness of the penalty coefficient settings in the model, this section conducts a sensitivity analysis on three key penalty coefficients based on the results of 30 Monte Carlo simulations, investigating their respective effects on the system's long-term cost rate and unavailability.

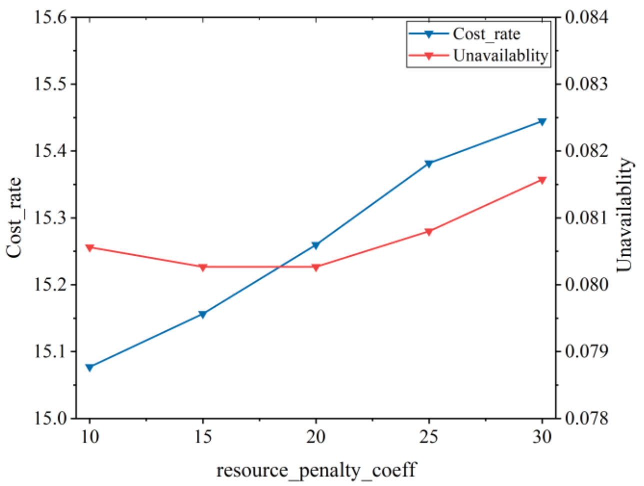

Figure 19. Sensitivity analysis of the resource penalty coefficient.

The analysis results for the resource shortage penalty coefficient are shown in Fig. 19. As the penalty coefficient increases, the system's long-term cost rate exhibits a significant monotonically increasing trend, and unavailability also increases gradually in tandem. This is because the higher the resource penalty coefficient, the stronger the model's constraints on resource overload maintenance behavior; to avoid high penalty costs, the algorithm tends to reduce the frequency of synchronous maintenance and increase the frequency of individual maintenance, leading to an increase in maintenance frequency and system downtime, which ultimately drives up the cost rate and unavailability.

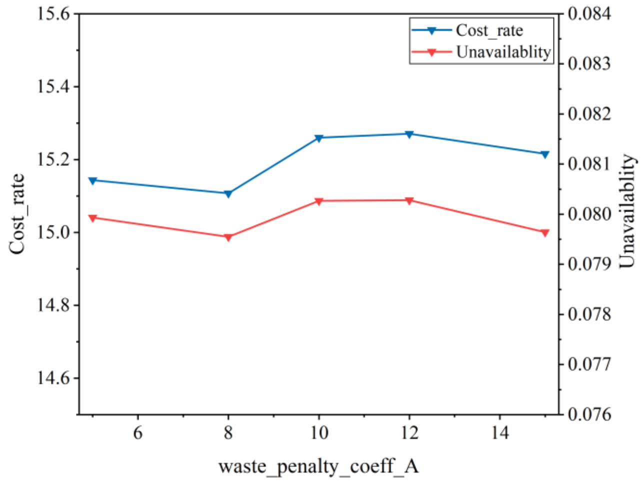

Figure 20. Sensitivity analysis of the penalty coefficient for component A.

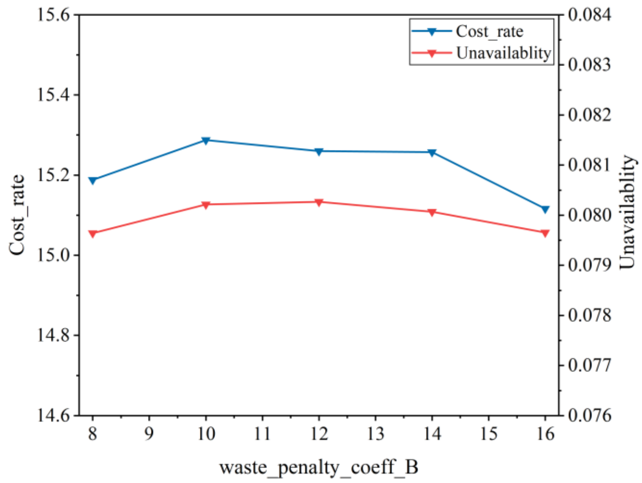

Figure 21. Sensitivity analysis of the penalty coefficient for component B.

The analysis of the lifetime waste penalty coefficient for Component A is shown in Fig. 20. Both the cost rate and unavailability exhibit a gradual trend, initially decreasing slightly before stabilizing, with no significant fluctuations.

When the coefficient varies within the range of 5–15, the fluctuation in the cost rate is less than 1.2%, and the change in unavailability is less than 1%. This indicates that the impact of this parameter on system performance is limited over a wide range, and the model demonstrates good robustness regarding its settings.

The influence pattern of the lifetime waste penalty coefficient for Component B is similar to that of Component A, as shown in Fig. 21. As the coefficient increases from 8 to 16, both the cost rate and unavailability exhibit only slight fluctuations, with the overall trend remaining stable and no sudden changes in performance occurring.

Based on the sensitivity analysis results for these three types of parameters, the penalty coefficient values selected in this study all fall within the performance stability range. Their impact on the system optimization objectives is moderate and controllable, demonstrating the rationality of the parameter settings and the robustness of the model, and providing a reliable basis for the engineering application of subsequent maintenance strategies.

5. Conclusion and future work

This paper investigates the optimization of maintenance strategies for systems composed of heterogeneous components, using a simple bidirectionally coupled heterogeneous component system as an example. Unlike other approaches, we focus on coupling relationships, economic dependencies, system lifespan, limited maintenance resources, and dual-objective optimization. A unified coupling degradation model is constructed at the physical level, employing distinct degradation models for heterogeneous components to describe complex coupling relationships. Concurrently, a grouped maintenance optimization model is established to minimize the long-term cost rate and unavailability of the system. Different maintenance strategies are selected for various components, accounting for penalty costs arising from premature maintenance and resource shortages due to grouped maintenance. A rolling time-domain approach based on the NSGA-II algorithm is proposed. Numerical simulations validate the effectiveness and advanced nature of the model and strategy, with a focus on analyzing coupling strength and economic dependency.

The numerical examples section validated the proposed coupling model through 30 simulation runs, yielding the optimal discount factor for the system under moderate coupling conditions: $\alpha_A^p = 0.736$, $\alpha_B^p = 0.777$ and $\beta_A^o = 0.713$, $\beta_B^o = 0.877$. At this point, the system's long-term cost rate and unavailability are 13.4902 and 0.07074, respectively. Moreover, compared to other strategies, S3 demonstrated improvements of approximately 26.99%, 10.29%, and 8.93% in long-term system cost rate and unavailability, respectively, alongside reductions of 29.13%, 15.25%, and 12.66% in long-term system cost rate and unavailability, proving the superiority of the proposed strategy. In coupling strength analysis, S3 consistently maintains the lowest long-term system cost rate and unavailability as coupling strength increases. In economic dependency analysis, as cost-saving factors increase, system components tend to be maintained collectively, thereby reducing both the long-term cost rate and unavailability of the system. Among these factors, cost-saving factors significantly impact the long-term cost rate, while time-saving factors substantially affect system unavailability. However, due to penalty constraints, neither factor benefits from being maximized, a trade-off must be made between gains and penalties.

In the parameter sensitivity analysis, we examined the effects of decision variables, inspection intervals, prediction windows, and penalty coefficients on the system's long-term cost rate and unavailability. In the analysis of decision variables, only the preventive maintenance discount factor A had a significant impact on system performance, while the effects of the remaining decision variables were weak or even insignificant, demonstrating the model's strong parameter robustness. There is a clear optimal range for inspection intervals: intervals that are too short increase inspection costs and lead to excessive maintenance, while intervals that are too long delay fault detection and increase the risk of failure. A moderate interval achieves the optimal balance between economic efficiency and reliability. The prediction window length also has an optimal value; if too short, it leads to short-sighted decision-making and insufficient grouping benefits, while if too long, it introduces prediction uncertainty and reduces decision-making flexibility. The window length selected in this study ensures optimization accuracy while maintaining efficient solution. Furthermore, the analysis of penalty coefficients indicates that the resource shortage penalty has a significant positive impact on the system cost rate, whereas the lifetime waste penalty has a negligible effect within a reasonable range, proving that the parameter settings in this study are reasonable and reliable. Overall, the proposed model and optimization strategy maintain stable and reliable optimization results within the reasonable fluctuation range of key parameters, demonstrating good engineering applicability and robustness.

From the perspective of practical engineering implementation, the proposed maintenance strategy can be deployed following a standard workflow: first, collecting real-time vibration and degradation state data through on-line monitoring sensors; second, calibrating model parameters based on historical failure and operation records; third, executing rolling horizon multi-objective optimization at each decision epoch to obtain optimal maintenance and grouping schemes; finally, arranging on-site maintenance tasks and coordinating limited repair resources according to the optimized results. The method is suitable for long-term operation and health management of coupled electromechanical equipment, and can be conveniently embedded into existing equipment maintenance management systems with good practical applicability and popularization value.

This paper uses a two-component system as an example to conduct research on maintenance optimization for heterogeneous multi-component systems. However, due to limitations in modeling complexity and engineering implementation, certain constraints remain: (1) The study focuses solely on two-component systems and has not yet been extended to more complex systems with additional components; (2) The model assumes ideal monitoring conditions and does not account for monitoring uncertainties such as measurement noise and observation errors; (3) Cost parameters and maintenance resource scheduling are treated as fixed values, without accounting for volatility, resulting in a certain discrepancy from actual industrial scenarios; (4) Due to practical constraints, the proposed strategy has not yet been validated through pilot testing in real industrial settings.

Given the aforementioned limitations, future research will focus on three areas: theoretical modeling, strategy expansion, and engineering implementation. First, we will construct a multi-component coupling matrix to extend the bidirectional coupling modeling method to complex multi-component systems with series and parallel structures, thereby accurately describing the coupling relationships among multi-dimensional heterogeneous components; Second, we will relax the ideal monitoring assumption by introducing monitoring uncertainty, random cost fluctuations, and dynamic resource allocation mechanisms, and integrating more realistic degradation models such as nonlinear vibration and variable load excitation; Third, we will extend the dynamic grouping maintenance framework to a multi-level scheduling system, designing heuristic or analytical solution algorithms tailored to complex constraints to improve solution efficiency for large-scale systems; Fourth, we will collaborate with manufacturing enterprises to conduct industrial pilot validations, optimizing models based on actual operational data to further enhance the engineering practicality and general applicability of the strategies.

The model proposed in this paper employs a modular design and offers excellent scalability. It can be continuously refined through iterative improvements in areas such as multi-component system topologies, diversified maintenance strategies, relaxed assumptions, and adaptation to industrial scenarios, thereby providing more general theoretical and technical support for intelligent maintenance decision-making in heterogeneous mechatronic systems.

References

1. Nicolai RP, Dekker R. Optimal Maintenance of Multi-component Systems: A Review. In: Kobbacy KAH, Murthy DNP, eds. Complex System Maintenance Handbook. London: Springer London; 2008. pp. 263–86. https://doi.org/10.1007/978-1-84800-011-7_11 doi:10.1007/978-1-84800-011-7_11.
2. Wildeman RE, Dekker R, Smit ACJM. A dynamic policy for grouping maintenance activities. *European Journal of Operational Research* 1997; 99(3): 530-51. doi:10.1016/S0377-2217(97)00319-6.
3. Wildeman RE, Dekker R. Dynamic influences in multi-component maintenance. *Quality and Reliability Engineering International* 1997; 13(4): 199-207. doi:10.1002/(SICI)1099-1638(199707)13:4<199::AID-QRE118>3.0.CO;2-A.

4. Van PD, Vu HC, Barros A, Berenguer C. Grouping maintenance strategy with availability constraint under limited repairmen. *IFAC Proceedings Volumes* 2012; 45(20): 486-91. doi:10.3182/20120829-3-MX-2028.00194.
5. Nguyen VT, Do P, Franciosi C, Voisin A, Iung B, Li L. Dynamic Grouping in Maintenance Planning and Optimization: an Industrial Application. *IFAC-PapersOnLine* 2024; 58(19): 504-9. doi:10.1016/j.ifacol.2024.09.262.
6. Xu J, Liu B, Zhao X, Wang XL. Online reinforcement learning for condition-based group maintenance using factored Markov decision processes. *European Journal of Operational Research* 2024; 315(1): 176-90. doi:10.1016/j.ejor.2023.11.039.
7. Do Van P, Barros A, Bérenguer C, Bouvard K, Brissaud F. Dynamic grouping maintenance with time-limited opportunities. *Reliability Engineering & System Safety* 2013; 120: 51-9. doi:10.1016/j.ress.2013.03.016.
8. Olde Keizer MCA, Flapper SDP, Teunter RH. Condition-based maintenance policies for systems with multiple dependent components: A review. *European Journal of Operational Research* 2017; 261(2): 405-20. doi:10.1016/j.ejor.2017.02.044.
9. Bafandegan Emroozi V, Kazemi M, Doostparast M. Enhancing industrial maintenance planning: Optimization of human error reduction and spare parts management. *Operations Research Perspectives* 2025; 14: 100336. doi:10.1016/j.orp.2025.100336.
10. Do P, Vu HC, Barros A, Bérenguer C. Maintenance grouping for multi-component systems with availability constraints and limited maintenance teams. *Reliability Engineering & System Safety* 2015; 142: 56-67. doi:10.1016/j.ress.2015.04.022.
11. Nguyen T, Deloux E, Dieullez L. Maintenance policies for a heterogeneous two-component system with stochastic and economic dependencies. *IFAC-PapersOnLine* 2016; 49(12): 787-92. doi:10.1016/j.ifacol.2016.07.870.
12. Zhang N, Fouladirad M, Barros A, Zhang J. Condition-based maintenance for a K-out-of-N deteriorating system under periodic inspection with failure dependence. *European Journal of Operational Research* 2020; 287(1): 159-67. doi:10.1016/j.ejor.2020.04.041.
13. Wang Y, Li X, Chen J, Liu Y. A condition-based maintenance policy for multi-component systems subject to stochastic and economic dependencies. *Reliability Engineering & System Safety* 2022; 219: 108174. doi:10.1016/j.ress.2021.108174.
14. Zhang Z, Wu S, Li B, Lee S. Optimal maintenance policy for multi-component systems under Markovian environment changes. *Expert Systems with Applications* 2013; 40(18): 7391-9. doi:10.1016/j.eswa.2013.07.003.
15. Huynh KT, Vu HC, Nguyen TD, Ho AC. A predictive maintenance model for k-out-of-n:F continuously deteriorating systems subject to stochastic and economic dependencies. *Reliability Engineering & System Safety* 2022; 226: 108671. doi:10.1016/j.ress.2022.108671.
16. Han Q, Ding Z, Xu X, Wang T, Chu F. Stator current model for detecting rolling bearing faults in induction motors using magnetic equivalent circuits. *Mechanical Systems and Signal Processing* 2019; 131: 554-75. doi:10.1016/j.ymssp.2019.06.010.
17. Hao J, Yao Z, Li C, Liu C, Hua C, Yu C, et al. Nonlinear electromechanical coupling integrated modeling and analysis of motorized spindle under mechanical and electromagnetic loads. *Nonlinear Dynamics* 2025; 113(11): 12817-66. doi:10.1007/s11071-025-10865-2.
18. Li Z, Cai R, Nie X. Experimental Study: Bearing Degradation Caused by Electrical Currents and Voltages at Low Speeds. *Lubricants* 2025; 13(4). doi:10.3390/lubricants13040175.
19. Song M, Liang Z. A hierarchical state ordering method for heterogeneous k-out-of-n:F systems with multi-state load-sharing components. *Reliability Engineering & System Safety* 2025; 262: 111167. doi:10.1016/j.ress.2025.111167.
20. Lu B, Wang X, Cui W, Ye Z. A predictive opportunistic maintenance policy for a serial–parallel multi-station manufacturing system with heterogeneous components. *Reliability Engineering & System Safety* 2025; 256: 110711. doi:10.1016/j.ress.2024.110711.
21. Kivanç İ, Fecarotti C, Raassens N, Van Houtum GJ. A scalable multi-objective maintenance optimization model for systems with multiple heterogeneous components and a finite lifespan. *European Journal of Operational Research* 2024; 315(2): 567-79. doi:10.1016/j.ejor.2023.12.005.
22. Bautista L, Castro IT, Landesa L. Maintenance cost assessment for heterogeneous multi-component systems incorporating perfect inspections and waiting time to maintenance. arXiv; 2024 [acessed 12 december 2025]. http://arxiv.org/abs/2401.11538 doi:10.48550/arXiv.2401.11538.
23. Bautista L, Castro IT, Nardo MD, Murino T. Condition-based and age-based maintenance in a multi-component system with heterogeneous components incorporating imperfect preventive maintenance actions. *Computers & Industrial Engineering* 2025; 206: 111188. doi:10.1016/j.cie.2025.111188.
24. Kıvanç İ, Fecarotti C, Raassens N, van Houtum GJ. Condition-based maintenance for multi-component systems: A scalable optimization model with two thresholds. *Reliability Engineering & System Safety* 2025; 254: 110634. doi:10.1016/j.ress.2024.110634.

25. Zhao Y, Cozzani V, Sun T, Vatn J, Liu Y. Condition-based maintenance for a multi-component system subject to heterogeneous failure dependencies. *Reliability Engineering & System Safety* 2023; 239: 109483. doi:10.1016/j.ress.2023.109483.
26. Zeng J, Liang Z. A dynamic predictive maintenance approach using probabilistic deep learning for a fleet of multi-component systems. *Reliability Engineering & System Safety* 2023; 238: 109456. doi:10.1016/j.ress.2023.109456.
27. He R, Tian Z, Wang Y, Zuo M, Guo Z. Condition-based maintenance optimization for multi-component systems considering prognostic information and degraded working efficiency. *Reliability Engineering & System Safety* 2023; 234: 109167. doi:10.1016/j.ress.2023.109167.
28. Geurtsen M, Leenen C, Adan I, Atan Z. Deep reinforcement learning for optimal planning of production line maintenance with deterioration. *Reliability Engineering & System Safety* 2026; 266: 111767. doi:10.1016/j.ress.2025.111767.
29. Tan S, Hu Q, Guo C, Zhu D, Dong E, Zhang F. Operational readiness-oriented condition-based maintenance and spare parts optimization for multi-state systems. *Reliability Engineering & System Safety* 2025; 264: 111367. doi:10.1016/j.ress.2025.111367.
30. Ma WN, Li H, Yang ZY, Hu QW. Maintenance Optimization for Two-Component Series Systems With Degradation Dependence. *IEEE Access* 2021; 9: 48174-84. doi:10.1109/ACCESS.2021.3062567.
31. Lu H, Yu M, Zhang B. Multistage Prognosis for Nonlinear Electromechanical Systems with Degradation Coupling and Maintenance. *IEEE Transactions on Industrial Informatics* 2024; 20(4): 6009-18. doi:10.1109/TII.2023.3342425.
32. Cui H, Tian W, Xu H, Wang H, Huang J, Peng C, et al. The Reliability of Complex Components under Temperature Cycling, Random Vibration, and Combined Loading for Airborne Applications. *Crystals* 2023; 13(3). doi:10.3390/cryst13030473.
33. Islam AMA, Vatn J. Condition-based multi-component maintenance decision support under degradation uncertainties. *International Journal of System Assurance Engineering and Management* 2023; 14(S4): 961-79. doi:10.1007/s13198-023-01900-9.
34. Cui L. Discussion of virtual age: Is it real? 2020 [acessed 6 december 2025]. https://onlinelibrary.wiley.com/doi/10.1002/asmb.2581.
35. Brenière L, Doyen L, Bérenguer C. Virtual age models with time-dependent covariates: A framework for simulation, parametric inference, and quality of estimation. *Reliability Engineering & System Safety* 2020; 203: 107054. doi:10.1016/j.ress.2020.107054.
36. Yang B, Huo J, Yang B, Huo J. A Multi-Level Nonlinear Cumulative Fatigue Damage Life Prediction Model Considering Load Loading Effects. *Materials* 2025; 18(17). doi:10.3390/ma18173973.
37. Liu X, Ma M. Cumulative fatigue damage theories for metals: review and prospects. *International Journal of Structural Integrity* 2023; 14(5): 629-62. doi:10.1108/ijsi-09-2022-0119.
38. Yi H, Zhang W, Wang G, Zhang X, Zhai Q. Statistical multivariate degradation modeling– A systematic review. *Reliability Engineering & System Safety* 2025; 264: 111286. doi:10.1016/j.ress.2025.111286.
39. Fang G, Pan R, Hong Y. Copula-based reliability analysis of degrading systems with dependent failures. *Reliability Engineering & System Safety* 2020; 193: 106618. doi:10.1016/j.ress.2019.106618.
40. Pan G, Ding X, Li D, Li Y, Wang Y. A reliability evaluation method of complex electromechanical products based on the multi-stress coupling acceleration model. *Engineering Failure Analysis* 2023; 146: 107115. doi:10.1016/j.engfailanal.2023.107115.
41. Saberzadeh Z, Razmkhah M. Reliability of degrading complex systems with two dependent components per element. *Reliability Engineering & System Safety* 2022; 222: 108398. doi:10.1016/j.ress.2022.108398.
42. Zheng Y, Zhang Y. Reliability analysis for systems with dependent components based on survival signature and copula theory. *Reliability Engineering & System Safety* 2023; 238: 109402. doi:10.1016/j.ress.2023.109402.
43. Castro IT, Landesa L. A dependent complex degrading system with non-periodic inspection times. arXiv; 2024 [acessed 6 december 2025]. http://arxiv.org/abs/2401.09141 doi:10.48550/arXiv.2401.09141.
44. Liu B, Pandey MD, Wang X, Zhao X. A finite-horizon condition-based maintenance policy for a two-unit system with dependent degradation processes. *European Journal of Operational Research* 2021; 295(2): 705-17. doi:10.1016/j.ejor.2021.03.010.
45. Zhang W, Zhang X, He S, Zhao X, He Z. Optimal condition-based maintenance policy for multi-component repairable systems with economic dependence in a finite-horizon. *Reliability Engineering & System Safety* 2024; 241: 109612. doi:10.1016/j.ress.2023.109612.
46. Do P, Assaf R, Scarf P, Iung B. Modelling and application of condition-based maintenance for a two-component system with stochastic and economic dependencies. *Reliability Engineering & System Safety* 2019; 182: 86-97. doi:10.1016/j.ress.2018.10.007.
47. Dekker R. Applications of maintenance optimization models; a review and analysis. *Reliability Engineering & Systems Safety* 1996; 51: 229-40. doi:10.1016/0951-8320(95)00076-3.

48. Wang H. A survey of maintenance policies for deteriorating systems. *European Journal of Operational Research* 2002; 139(3): 469-89. doi:10.1016/S0377-2217(01)00197-7.
49. Chang F, Zhou G, Zhang C, Xiao Z, Wang C. A service-oriented dynamic multi-level maintenance grouping strategy based on prediction information of multi-component systems. *Journal of Manufacturing Systems* 2019.
50. Di Nardo M, Murino T, Cammardella A, Wu J, Song M. Catalyzing industrial evolution: A dynamic maintenance framework for Maintenance 4.0 optimization. *Computers & Industrial Engineering* 2024; 196: 110469. doi:10.1016/j.cie.2024.110469.
51. Shi Y, Zhu W, Xiang Y, Feng Q. Condition-based maintenance optimization for multi-component systems subject to a system reliability requirement. *Reliability Engineering & System Safety* 2020; 202: 107042. doi:10.1016/j.ress.2020.107042.
52. Gutierrez-Miravete E. Determination of the Optimal Replacement Age for the Preventive Maintenance of Bearing Assemblies Involving Weibull Failure Probability Distribution Functions. *Universal Journal of Mechanical Engineering* 2020; 8(6): 287-97. doi:10.13189/ujme.2020.080601.
53. Wang Y, Wang G, Wu Y, Zhang G, Zheng R. Optimal predictive maintenance for a nonstationary gamma process. *Eksploatacja i Niezawodnosc - Maintenance and Reliability* 2025; 27(4). http://doi.org/10.17531/ein/203543.
54. Vu HC, Do P, Barros A, Bérenguer C. Maintenance grouping strategy for multi-component systems with dynamic contexts. *Reliability Engineering & System Safety* 2014; 132: 233-49. doi:10.1016/j.ress.2014.08.002.

Parameter	**Notation**
$i \in \{A, B\}$	component collection
C_i^p, C_i^c	cost of preventive and corrective maintenance of component i respectively
C_G	cost savings of group maintenance
a, b	cost and time saving factors for group maintenance
c_d	downtime cost-rate of the system
d_i^p, d_i^c	duration of a preventive and corrective maintenance for component i， respectively
$C_{ins,i}$	cost of inspection of component i
τ	the time interval of the inspection of the system
T_A^c, D_B^c	failure threshold of component A and B, respectively
$T_A^p, D_B^p, T_A^o, D_B^o$	preventive and group maintenance thresholds for component A and B, respectively
α_i^p, β_i^o	preventive and group maintenance discount factors for component i, respectively
r_i^p， r_i^c	the demand for preventive and corrective maintenance resources of component i, respectively
c_i^w, c_r	penalty coefficient